Impact of Timanian thrust systems on the late Neoproterozoic–Phanerozoic tectonic evolution of the Barents Sea and Svalbard

Jean-Baptiste P. Koehl[1,2,3,4], Craig Magee[5], Ingrid M. Anell[6]

[1]Centre for Earth Evolution and Dynamics (CEED), University of Oslo, PO Box 1028 Blindern, N-0315 Oslo, Norway.

[2]Department of Geosciences, UiT The Arctic University of Norway in Tromsø, N-9037 Tromsø, Norway.

[3]Research Centre for Arctic Petroleum Exploration (ARCEx), UiT The Arctic University of Norway in Tromsø, N-9037 Tromsø, Norway.

[4]CAGE – Centre for Arctic Gas Hydrate, Environment and Climate, UiT The Arctic University of Norway in Tromsø, N-9037 Tromsø, Norway.

[5]School of Earth Science and Environment, University of Leeds, Leeds, LS2 9JT, United Kingdom.

[6]Department of Geosciences, University of Oslo, P.O. Box 1047 Blindern, N-0316 Oslo, Norway.

Correspondence: Jean-Baptiste P. Koehl (jean-baptiste.koehl@uit.no)

Abstract

The Svalbard Archipelago consists of three basement terranes that record a complex Neoproterozoic–Phanerozoic tectonic history, including four contractional events (Grenvillian, Caledonian, Ellesmerian, and Eurekan) and two episodes of collapse- to rift-related extension (Devonian–Carboniferous and late Cenozoic). Previous studies suggest these three terranes likely accreted during the early–mid Paleozoic Caledonian and Ellesmerian orogenies. Yet recent geochronological analyses show that the northwestern and southwestern terranes of Svalbard both record an episode of amphibolite (–eclogite) facies metamorphism in the latest Neoproterozoic, which may relate to the 650–550 Ma Timanian Orogeny identified in northwestern Russia, northern Norway and the Russian Barents Sea. However, discrete Timanian structures have yet to be identified in Svalbard and the Norwegian Barents Sea. Through analysis of seismic reflection, and regional gravimetric and magnetic data, this study demonstrates the presence of continuous, several kilometers thick, NNE-dipping, deeply buried thrust systems that extend thousands of kilometers from northwestern Russia to northeastern Norway, the northern Norwegian Barents Sea, and the Svalbard Archipelago. The consistency in orientation and geometry, and apparent linkage between

32   these thrust systems and those recognized as part of the Timanian Orogeny in northwestern Russia

33   and Novaya Zemlya suggests that the mapped structures are likely Timanian. If correct, these

34   findings would imply that Svalbard's three basement terranes and the Barents Sea were accreted

35   onto northern Norway during the Timanian Orogeny and should, hence, be attached to Baltica and

36   northwestern Russia in future Neoproterozoic–early Paleozoic plate tectonics reconstructions. In

37   the Phanerozoic, the study suggests that the interpreted Timanian thrust systems represented major

38   preexisting zones of weakness that were reactivated, folded, and overprinted by (i.e., controlled the

39   formation of new) brittle faults during later tectonic events. These faults are still active at present

40   and can be linked to folding and offset of the seafloor.

Introduction

43   Recognizing and linking tectonic events across different terranes is critical to plate

44   reconstructions. In the latest Neoproterozoic (at ca. 650–550 Ma), portions of northwestern Russia

45   (e.g., Timan Range and Novaya Zemlya) and the Russian Barents Sea were accreted to northern

46   Baltica by top-SSW thrusting during the Timanian Orogeny (Olovyanishnikov et al., 2000;

47   Kostyuchenko et al., 2006). Discrete Timanian structures with characteristic WNW–ESE strikes

48   are sub-orthogonal to the N–S-trending Caledonian grain formed during the closure of the Iapetus

49   Ocean (Gee et al., 1994; Witt-Nilsson et al., 1998; Johansson et al., 2004; 2005). Thus far,

50   Timanian structures have only been identified in onshore–nearshore areas of northwestern Russia

51   and northeastern Norway and offshore in the Russian Barents Sea and southeasternmost Norwegian

52   Barents Sea (Barrère et al., 2009, 2011; Marello et al., 2010; Gernigon et al., 2018; Hassaan et al.,

53   2020a, 2020b, 2021; Hassaan, 2021). Therefore, the nature of basement rocks in the northern and

54   southwestern Norwegian Barents Sea remains debatable. Some studies suggest a NE–SW-trending

55   Caledonian suture within the Barents Sea (Gudlaugsson et al., 1998; Gee and Teben'kov, 2004;

56   Breivik et al., 2005; Gee et al., 2008; Knudsen et al., 2019), whereas others argue for a swing into

57   a N–S trend and merging of Norway and Svalbard's Caledonides, which probably continue into

58   northern Greenland (Ziegler, 1988; Gernigon and Brönner, 2012; Gernigon et al., 2014).

59   Regardless, these models solely relate basement structures in the northern and southwestern

60   Norwegian Barents Sea to the Caledonian Orogeny, implying that Laurentia and Svalbard were not

61   involved in the Timanian Orogeny and were separated from Baltica by the Iapetus Ocean in the

62 latest Neoproterozoic (Torsvik and Trench, 1991; Cawood et al., 2001; Cocks and Torsvik, 2005;
63 Torsvik et al., 2010; Merdith et al., 2021).

64   Nonetheless, geochronological data yielding Timanian ages suggest that deformation and
65 metamorphism contemporaneous of the Timanian Orogeny affected parts of the Svalbard
66 Archipelago and Laurentia and, possibly, all Arctic regions (Estrada et al., 2018; Figure 1a): (1)
67 eclogite facies metamorphism (620–540 Ma; Peucat et al., 1989; Dallmeyer et al., 1990b) and
68 eclogite facies xenoliths of mafic–intermediate granulite in Quaternary volcanic rocks are found in
69 northern Spitsbergen (648–556 Ma; Griffin et al., 2012); (2) amphibolite facies metamorphism
70 (643 ± 9 Ma; Majka et al., 2008, 2012, 2014; Mazur et al., 2009) and WNW–ESE-striking shear
71 zones like the Vimsodden–Kosibapasset Shear Zone (VKSZ; Figure 1b–c) occur in southwestern
72 Spitsbergen (600–537 Ma; Manecki et al., 1998; Faehnrich et al., 2020); and (3) xenoliths of the
73 subduction-related Midtkap igneous suite in northern Greenland yield Timanian ages (628–570
74 Ma; Rosa et al., 2016; Estrada et al., 2018). In addition, several recent studies also show the
75 presence of NW–SE- to E–W-trending basement grain in the Norwegian Barents Sea, which could
76 possibly represent Timanian fabrics and structures (Figure 1b; Barrère et al., 2009, 2011; Marello
77 et al., 2010; Klitzke et al., 2019). Following these developments, a few paleo-plate reconstructions
78 now place Svalbard together with Baltica in the latest Neoproterozoic–Paleozoic (e.g.,
79 Vernikovsky et al., 2011), and imply that the Norwegian Barents Sea and Svalbard basement may
80 contain Timanian structures overprinted during later (e.g., Caledonian) deformation events.

81   To test the origin of basement grain in the northern Norwegian Barents Sea and Svalbard,
82 the present study focuses on several kilometers deep structures identified on 2D seismic reflection
83 data and correlated using regional gravimetric and magnetic data. These newly identified structures
84 trend WNW–ESE, i.e., parallel to the Timanian structural grain in northwestern Russia and
85 northern Norway (Figure 1a–c). The structures are described and interpreted based on their
86 geometry and potential kinematic indicators, and are compared to well-known examples of
87 Caledonian and Timanian fabrics and structures elsewhere, e.g., onshore Norway (e.g., NNE-
88 dipping Trollfjorden–Komagelva Fault Zone – TKFZ; Siedlecka and Siedlecki, 1967; Siedlecka,
89 1975), in Svalbard (e.g., gently north-plunging Atomfjella Antiform – AA; Witt-Nilsson et al.,
90 1998), in northwestern Russia (NNE-dipping Central Timan Fault – CTF – and related Mikulkin
91 Antiform; Siedlecka and Roberts, 1995; Olovyanishnikov et al., 2000; Lorenz et al., 2004;
92 Kostyuchenko et al., 2006), and in the southern Norwegian Barents Sea (Barrère et al., 2011;

93   Gernigon et al., 2014) and the Russian Barents Sea (NNE-dipping Baidaratsky fault zone – BaFZ;

94   Lopatin et al., 2001; Korago et al., 2004; Figure 1b–c). The present contribution proposes a scenario

95   involving several episodes of deformation starting in the Timanian Orogeny, and involving

96   reactivation and overprinting of Timanian structures during the Caledonian Orogeny, Devonian–

97   Carboniferous extension, Triassic extension, Eurekan tectonism, and present-day tectonism.

98   Having established that Timanian structure may be present across the Barents Sea and Svalbard,

99   we briefly discuss the potential implications for the tectonic evolution of the Barents Sea and the

100   Svalbard Archipelago and associated basins (e.g., Ora and Olga basins; Anell et al., 2016).

101   Should our interpretation of discrete Timanian structures throughout the Norwegian

102   Barents Sea and Svalbard be validated by future research, it would support accretion of these

103   terranes to Baltica in the late Neoproterozoic and place the Caledonian suture farther west than is

104   commonly suggested (e.g., Breivik et al., 2005; Gernigon et al., 2014), thus leading to a major

105   revision of plate tectonics models. In addition, constraining the extent and reactivation history of

106   such faults may shed some light on their influence on younger tectonic events, such as Caledonian,

107   Ellesmerian and Eurekan contraction, Devonian–Carboniferous collapse–rifting, and late Cenozoic

108   breakup and ongoing extension.

109

110   **Geological setting**

111   *Timanian Orogeny*

112   The Timanian Orogeny corresponds to a ca. 650–550 Ma episode of NNE–SSW

113   contractional deformation that affected northwestern Russia and northeastern Norway. During this

114   tectonic episode, crustal-scale, WNW–ESE-striking, NNE-dipping thrusts systems with south-

115   southwestwards transport direction (top-SSW; Siedlecka and Siedlecki, 1967; Siedlecka, 1975;

116   Figure 1b), accreted portions of the Russian Barents Sea and northwestern Russia onto northeastern

117   Baltica, including Novaya Zemlya, Severnaya Zemlya, the Kanin Peninsula, the Timan Range, and

118   the Kola Peninsula (Siedlecka and Roberts, 1995; Olovyanishshnikov et al., 2000; Roberts and

119   Siedlecka, 2002; Gee and Pease, 2004; Kostyuchenko et al., 2006; Lorenz et al., 2008; Marello et

120   al., 2013) and the Varanger Peninsula in northeastern Norway (Siedlecka and Siedlecki, 1967;

121   Siedlecka, 1975; Roberts and Olovyanishshnikov, 2004; Herrevold et al., 2009; Drachev, 2016;

122   Figure 1a). Major Timanian thrusts include the NNE-dipping Baidaratsky fault zone in the Russian

123   Barents Sea and Novaya Zemlya (Figure 1a–b; Eldholm and Ewing, 1971, their figure 4 profile C–

124 D; Lopatin et al., 2001; Korago et al., 2004; Drachev, 2016), the NNE-dipping Central Timan Fault

125 (and associated thrust anticline, the Mikulkin Antiform) on the Kanin Peninsula and the Timan

126 Range (Siedlecka and Roberts, 1995; Olovyanishnikov et al., 2000; Lorenz et al., 2004;

127 Kostyuchenko et al., 2006), and the NNE-dipping Trollfjorden–Komagelva Fault Zone in northern

128 Norway (Siedlecka and Siedlecki, 1967; Siedlecka, 1975; Herrevold et al., 2009).

129

130 ***Accretion of Svalbard basement terranes in the early Paleozoic***

131   The Svalbard Archipelago consists of three Precambrian basement terranes (Figure 2),

132 some of which show affinities with Greenland (northwestern and northeastern terranes), whereas

133 others are possibly derived from Pearya (southwestern terrane; Harland and Wright, 1979; Ohta et

134 al., 1989; Gee and Teben'kov, 2004; Labrousse et al., 2004; Piepjohn et al., 2013; Fortey and

135 Bruton, 2013). These terranes possibly accreted during the mid-Paleozoic Caledonian (collision of

136 Greenland with Svalbard and Norway at ca. 460–410 Ma; Horsfield, 1972; Dallmeyer et al., 1990a;

137 Johansson et al., 2004, 2005; Faehnrich et al., 2020) and Late Devonian Ellesmerian orogenies

138 (Piepjohn, 2000; Majka and Kosminska, 2017). In these models, accretion was facilitated via

139 hundreds of kilometers of displacement along (arcuate) N–S-striking strike-slip faults, such as the

140 Billefjorden Fault Zone (BFZ – Harland, 1969; Harland et al., 1992; Labrousse et al., 2008) and

141 the Lomfjorden Fault Zone (LFZ – Piepjohn et al., 2019; Figure 2), although other studies suggest

142 more limited strike-slip displacement (Lamar et al., 1986; Manby and Lyberis, 1992; Manby et al.,

143 1994; Lamar and Douglass, 1995). Some previous workers assumed that these large (strike-slip?)

144 faults extended thousands of kilometers southwards and represented the continuation of Caledonian

145 faults in Scotland (Norton et al., 1987; Dewey and Strachan, 2003). Caledonian contraction resulted

146 in the formation of large fold and thrust complexes, such as the N–S-trending, gently north-

147 plunging Atomfjella Antiform in northeastern Spitsbergen (Gee et al., 1994; Witt-Nilsson et al.,

148 1998) and the N–S-trending Rijpdalen Anticline in Nordaustlandet (Johansson et al., 2004; 2005;

149 Dumais and Brönner, 2020), whereas Ellesmerian tectonism may have formed narrow N–S-

150 trending fold and thrust belts, like the Dickson Land and Germaniahalvøya fold-thrust zones

151 (McCann, 2000; Piepjohn, 2000; Dallmann and Piepjohn, 2020).

152   In northern Norway, Timanian thrusts were reactivated–overprinted in subsequent tectonic

153 events (e.g., Caledonian Orogeny and late–post-Caledonian collapse–rifting) as dominantly strike-

154 to oblique-slip faults (Siedlecka and Siedlecki, 1971; Roberts et al., 1991; Herrevold et al., 2009;

Rice, 2014). A notable example is the folding and reactivation of Timanian fabrics and structures (e.g., NNE-dipping Trollfjorden–Komagelva Fault Zone) during the Caledonian Orogeny (Siedlecka and Siedlecki, 1971; Herrevold et al., 2009) and intrusion of Mississippian dolerite dykes along steeply dipping WNW–ESE-striking brittle faults that overprint the Trollfjorden–Komagelva Fault Zone onshore–nearshore northern Norway (Roberts et al., 1991; Lippard and Prestvik, 1997; Nasuti et al., 2015; Koehl et al., 2019).

Late Paleozoic post-Caledonian collapse and rifting

In the latest Silurian–Devonian, extensional collapse of the Caledonides led to the deposition of several kilometers thick sedimentary basins such as the Devonian Graben in northern Spitsbergen (Gee and Moody-Stuart, 1966; Friend et al., 1966; Friend and Moody-Stuart, 1972; Murascov and Mokin, 1979; Manby and Lyberis, 1992; Manby et al., 1994; Friend et al., 1997; McCann, 2000; Dallmann and Piepjohn, 2020). In places, N–S-trending basement ridges potentially exhumed as metamorphic core complexes along bowed, reactivated detachments, such as the Keisarhjelmen Detachment in northwestern Spitsbergen (Braathen et al., 2018).

In the latest Devonian–Mississippian, coal-rich sedimentary strata of the Billefjorden Group were deposited within normal fault-bounded basins throughout Spitsbergen (Cutbill and Challinor, 1965; Harland et al., 1974; Cutbill et al., 1976; Aakvik, 1981; Koehl and Muñoz-Barrera, 2018; Koehl, 2020a) and the Norwegian Barents Sea (Koehl et al., 2018a; Tonstad, 2018). As rift-related normal faulting evolved, Pennsylvanian sedimentation was localized into a few, several kilometers deep, N–S-trending basins like the Billefjorden Trough (Cutbill and Challinor, 1965; Braathen et al., 2011; Koehl et al., 2021 in review) and the E–W-trending Ora Basin (Anell et al., 2016). In the Permian, rift-related faulting stopped and platform carbonates were deposited throughout Svalbard (Cutbill and Challinor, 1965) and the Barents Sea (Larssen et al., 2005).

Overall, the several kilometers thick, late Paleozoic sedimentary succession deposited during late–post-Caledonian extension buried Proterozoic basement rocks. As a result, these rocks are sparsely exposed and, thus, difficult to study.

Mesozoic sedimentation and magmatism

In the Mesozoic, Svalbard and the Barents Sea remained tectonically quiet and were only affected by minor Triassic normal faulting (e.g., Anell et al., 2013; Osmundsen et al., 2014; Ogata

et al., 2018; Smyrak-Sikora et al., 2020). In the Early Cretaceous, Svalbard was affected by a regional episode of magmatism recorded by the intrusion of numerous dykes and sills of the Diabasodden Suite (Senger et al., 2013).

Early Cenozoic Eurekan tectonism

The opening of the Labrador Sea and Baffin Bay between Greenland and Arctic Canada in the early Cenozoic (Chalmers and Pulvercraft, 2001; Oakey and Chalmers, 2012) led to the collision of northern Greenland with Svalbard and the formation of a fold-and-thrust belt with top-east thrusts and east-verging folds in western Spitsbergen (Dallmann et al., 1993). In eastern Spitsbergen, this deformation event is characterized by dominantly thin-skinned deformation structures, including décollements, some of which showing westwards transport directions (Andresen et al., 1992; Haremo and Andresen, 1992). Notably, the N–S-striking Agardhbukta Fault, a major splay/segment of the N–S-striking Lomfjorden Fault Zone, accommodated reverse and, possibly, strike-slip movements during this event (Piepjohn et al., 2019).

Late Cenozoic opening of the Fram Strait

After the end of extension in the Labrador Sea and Baffin Bay, the Fram Strait started to open in the earliest Oligocene (Engen et al., 2008). Tectonic extension and break-up in the Fram Strait resulted in the formation of two major, NW–SE-striking transform faults (Lowell, 1972; Thiede et al., 1990; Figure 1b).

Methods and datasets

Seismic surveys from the DISKOS database (see Figure 1b–c and supplement S1 for location) were used to interpret basement-seated structures and related, younger, brittle overprints (Figure 3a–f and Figure 4a–h and supplement S2). Other features of interest include potential dykes, which commonly appear as high positive reflections on seismic data. The geology interpreted from onshore seismic data was directly correlated to geological maps of the Norwegian Polar Institute (e.g., Dallmann, 2015). Where possible, interpretation of offshore seismic data was tied to onshore geological maps and to exploration wells Raddedalen-1 and Plurdalen-1 on Edgeøya (Bro and Shvarts, 1983; Harland and Kelly, 1997) and to the Hopen-2 well on Hopen (Anell et al., 2014; Figure 1c and supplement S3). The Raddedalen-1 well penetrated 2823 meters

of Upper Permian to Mississippian or Ordovician strata, the Plurdalen well 2351 meters of Middle Triassic to (pre-?) Devonian strata, and the Hopen-2 well 2840 meters of Middle–Upper Triassic to Pennsylvanian strata (Bro and Shvarts, 1983; Harland and Kelly, 1997; Anell et al., 2014; Senger et al., 2019). Note that the present contribution favors interpretation of lower Paleozoic (Ordovician–Silurian) rocks in the Raddedalen-1 well by Bro and Shvarts (1983) to that of upper Paleozoic (Upper Devonian–Mississippian) by Cambridge Svalbard Exploration (see contrasting interpretations in Harland and Kelly, 1997). This is based on the more detailed lithological, palynological and paleontological analyses by the former, and on the strong contrast of the lithologies described in the well with Devonian–Mississippian successions on Svalbard (Cutbill and Challinor, 1965; Cutbill et al., 1976; Friend et al., 1997; Dallmann and Piepjohn, 2020).

The present contribution only includes a few examples of seismic sections. However, more interpreted and uninterpreted seismic data are available as supplements (supplements S1–2) and from the Norwegian Petroleum Directorate (DISKOS database). None of the seismic sections were depth-converted, and thicknesses therefore appear in seconds (Two-Way Time; TWT). However, local time conversion was performed to tie seismic wells onshore Edgeøya to seismic section in Storfjorden and depth conversion was performed locally to evaluate fault displacement. Velocities of Gernigon et al. (2018) were used in these conversions. Supplement S3 includes further details related to these conversions.

The boundary between Precambrian, lower Paleozoic and upper Paleozoic successions offshore are interpreted as major unconformities that truncate underlying reflections and fold structures (e.g., Figure 3a, b and c). The boundaries between Devonian–Permian and Mesozoic successions were tied to the Raddedalen-1, Plurdalen-1, and Hopen-2 exploration wells for offshore parts of the study area. The boundary between Devonian–Mississippian and Pennsylvanian–Permian onshore Svalbard are interpreted as a major unconformity truncating Devonian–Mississippian dykes (see Figure 3e).

The correlation of kilometer-thick structures discussed in the present contribution was also tested using gravimetric and magnetic data in cross section (Figure 3a–f) and regional magnetic and gravimetric data in the northern Norwegian Barents Sea and Svalbard (Figure 5 and supplement S4) from the Federal Institute for Geosciences and Natural Resources in Germany in map view (Klitzke et al., 2019). Regional gravimetric and magnetic data are also used to interpret deep basement fabrics and structures, e.g., regional folds (gravimetric highs commonly associated with

248   major anticlines of thickened dense basement with high metamorphic grade (i.e., Precambrian)

249   rocks (e.g., Mikulkin Antiform; Lorenz et al., 2004; Kostyuchenko et al., 2006) and gravimetric

250   lows with synclines with less dense sedimentary basins) and large faults bounding magmatic

251   complexes and/or intruded by magmatic bodies that commonly correlate with elongated

252   gravimetric and/or magnetic anomalies (e.g., Kostyuchenko et al., 2006; Koehl et al., 2019), and

253   to discuss the relationship of the described structures with known structural trends in onshore

254   basement rocks in Russia, Norway and Svalbard. Magnetic and gravimetric anomalies not related

255   to Timanian and Caledonian grains will not be discussed in the present study.

256

Results and interpretations

258   First, the interpretation of seismic data are described by area, including (1) Storfjorden

259   (between Edgeøya and Spitsbergen) and the northeastern part of the Norwegian Barents Sea (east

260   of Edgeøya), (2) Nordmannsfonna to Sassenfjorden onshore–nearshore the eastern–central part of

261   Spitsbergen, and (3) the northwestern part of the Norwegian Barents Sea between Bjørnøya and

262   Spitsbergen (Figure 1b–c). Description in each area starts with deep Precambrian basement rocks

263   and shallow sedimentary rock units, and ends with deep brittle–ductile structures and with shallow

264   brittle faults. Then, potential field data and regional gravimetric and magnetic anomalies in the

265   Barents Sea and Svalbard are described, and compared and correlated to seismic data and to major

266   Timanian and Caledonian fabrics and structures onshore northwestern Russia, Svalbard and

267   Norway. Please see high resolution versions of all the figures and supplements on DataverseNO

268   (doi.org/10.18710/CE8RQH).

269

Structures in the northwestern–northeastern Norwegian Barents Sea, Storfjorden and central–eastern Spitsbergen

272   *Storfjorden and northeastern Norwegian Barents Sea*

273   Folded Precambrian–lower Paleozoic basement rocks

274   Seismic facies at depths of 2–6 seconds (TWT) typically comprise successions of laterally

275   discontinuous (< three kilometers long), sub-horizontal, moderately curving–undulating,

276   moderate–high-amplitude seismic reflections that alternate with packages of highly-disrupted

277   and/or curved low-amplitude seismic reflections (see yellow lines within pink and purple units in

278   Figure 3a and Figure 4a). The curving geometries of the moderate–high amplitude reflections

279 display a typical kilometer- to hundreds of meter-scale wavelength and are commonly asymmetric,

280 seemingly leaning/verging towards the south/SSW (see yellow lines in Figure 4b). Based on ties

281 with well bores on Edgeøya (Raddedalen-1 well; Bro and Shvarts, 1983; Harland and Kelly, 1997),

282 these asymmetric, undulate features most likely correspond to SSW-verging folds in Precambrian–

283 lower Paleozoic basement rocks. In places, apparent reverse offsets of these undulate reflections

284 align along moderately–gently north- to NNE-dipping surfaces (see red lines in Figure 4a and c),

285 which are therefore interpreted as minor, top-south/SSW, brittle thrusts.

286 Upper Paleozoic–Mesozoic sedimentary successions

287   In Storfjorden and the northwestern Norwegian Barents Sea, shallow (0–3 seconds TWT)

288 seismic reflections above folded and thrust Precambrian–lower Paleozoic basement rocks show

289 significantly more continuous patterns (>> five kilometers), gently curving–undulating geometries

290 and only local disruptions by shallow, dominantly NNE-dipping, high-angle listric disruptions (see

291 yellow lines within orange unit in Figure 3a and c). In the northeastern Barents Sea, these

292 reflections are largely flat-lying (see yellow lines within orange unit in Figure 3b and d). Based on

293 field mapping campaigns and well-bores in adjacent onshore areas of Spitsbergen, Edgeøya, Hopen

294 and Bjørnøya (see location in Figure 1b), these continuous reflections are interpreted as mildly

295 folded upper Paleozoic–Mesozoic (–Cenozoic?) sedimentary strata (Dallmann and Krasil'scikov,

296 1996; Harland and Kelly, 1997; Worsley et al., 2001; Dallmann, 2015). The Permian–Triassic

297 boundary was correlated throughout the northern Norwegian Barents Sea and Storfjorden by using

298 the tie of Anell et al. (2014) to the Hopen-2 well.

299 Deep thrust systems

300   The packages of sub-horizontal, moderately curving–undulating (folded Precambrian–

301 lower Paleozoic basement) reflections alternate laterally from north to south with 20–60 kilometers

302 wide, up to four seconds thick (TWT), upwards-thickening, wedge-shaped packages (areas with

303 high concentrations of black lines in Figure 3a and d). These wide upwards-thickening packages

304 consist of two types of reflections. First, they include planar, continuous, gently–moderately north-

305 to NNE-dipping, sub-parallel, high-amplitude reflections that commonly merge together

306 downwards and that can be traced and correlated on several seismic sections in Storfjorden (black

307 lines in Figure 3a). Upwards, these reflections terminate against high-amplitude convex-upwards

308 reflections interpreted as intra- Precambrian–lower Paleozoic basement reflections (fuchsia lines

309 in Figure 3a and c) or continue as moderately NNE-dipping disruption surfaces that offset these

310 intra-basement reflections top-SSW (e.g., offset intra-Precambrian unconformities in Figure 3a and

311 c and Figure 4d).

312   Second, sub-parallel, high-amplitude reflections bound wedge-shaped, upwards-thickening

313 packages of asymmetric, curved, south- to SSW-leaning, moderately north- to NNE-dipping,

314 moderate-amplitude reflections showing narrow (< one kilometer wide) upwards-convex

315 geometries (Figure 4d). These asymmetric reflections also commonly appear as gently north- to

316 NNE-dipping packages of Z-shaped reflections bounded by sub-parallel, planar, high-amplitude

317 reflections (see yellow lines in Figure 4e). Asymmetric, south- to SSW-leaning, convex-upwards

318 reflections are interpreted as south- to SSW-verging fold anticlines reflecting relatively low

319 amounts of plastic deformation of layered rocks.

320   The alternation of packages of layered rocks folded into SSW-verging folds (yellow lines

321 in Figure 3a–c) with packages of planar, NNE-dipping, sub-parallel, high-amplitude reflections

322 (black lines in Figure 3a–c) suggest that the latter reflection packages represent zones where initial

323 layering was destroyed and/or possibly reoriented, i.e., areas that accommodated larger amounts of

324 deformation and tectonic displacement. Thus, planar, gently–moderately north- to NNE-dipping,

325 high-amplitude reflections (black lines in Figure 3a–c) are interpreted as low-angle brittle–ductile

326 thrust systems. We name these thrust systems (from north to south) the Steiløya–Krylen (SKFZ),

327 Kongsfjorden–Cowanodden (KCFZ), Bellsundbanken (BeFZ), and Kinnhøgda–Daudbjørnpynten

328 fault zones (KDFZ; Figure 3a and supplement S2a–b; see Figure 1c for location of the thrusts).

329   The relatively high-amplitude character of planar, NNE-dipping reflections within the

330 thrusts suggest that these tectonic structures consist of sub-parallel layers of rocks and minerals

331 with significantly different physical properties. A probable explanation for such laterally

332 continuous and consistently high-amplitude reflections is partial recrystallization of rocks layers–

333 mineral bands into rocks and minerals with significantly higher density along intra-thrust planes

334 that accommodated large amounts of displacement (e.g., mylonitization; Fountain et al., 1984;

335 Hurich et al., 1985). In places, packages of aggregates of Z-shaped reflections bounded upwards

336 and downwards by individual low-angle thrust surfaces are interpreted as forward-dipping duplex

337 structures (e.g., Boyer and Elliott, 1982) reflecting relatively strong plastic deformation between

338 low-angle, brittle–ductile (mylonitic?) thrusts (see yellow lines in Figure 4e).

339   The Kongsfjorden–Cowanodden, Bellsundbanken, and Kinnhøgda–Daudbjørnpynten fault

340 zones can be traced east-southeast of Edgeøya as a similar series of 20–60 kilometers wide, up to

341   four seconds thick (TWT), upwards-thickening packages (e.g., black lines in Figure 3d and

342   supplements S2a). However, their imaging along NNW–SSE-trending seismic sections is much

343   more chaotic and it is more difficult to identify smaller structures (like south-verging folds and

344   minor thrusts) within each thrust system (e.g., supplement S2a). This suggests that these three thrust

345   systems strike oblique to NNW–SSE-trending seismic sections (supplement S2a), whereas they are

346   most likely sub-orthogonal to N–S- to NNE–SSW-trending seismic sections in Storfjorden (Figure

347   3a). The only orientation that reconciles these seismic facies variations (i.e., well-imaged on NNE–

348   SSW-trending seismic sections and poorly imaged by NNW–SSE-trending seismic sections;

349   Figure 3a and supplement S2a) is an overall WNW–ESE strike.

350   South of each 20–60 kilometers wide packages of thrust surfaces and related fold and

351   duplex structures, seismic reflections representing Precambrian–lower Paleozoic basement rocks

352   typically appear as gently curved, convex-upwards, relatively continuous reflections showing sub-

353   horizontal seismic onlaps (see white arrows in Figure 3a–f). This suggests that Precambrian–lower

354   Paleozoic basement rocks most likely consist (meta-) sedimentary rocks (analogous to those

355   observed in northeastern Spitsbergen and Nordaustlandet; Harland et al., 1993; Stouge et al., 2011)

356   that were deposited in foreland and piggy-back basins ahead of each 20–60 kilometers wide

357   packages (Figure 3a–f).

358   Hence, based on the upwards-thickening geometry of the packages of south- to SSW-

359   verging folds and of forward-dipping duplexes, on the top-SSW reverse offsets of intra-basement

360   reflections by low-angle brittle–ductile thrust surfaces, on the upwards truncation of these low-

361   angle thrusts by intra-basement reflections, and on the onlapping geometries of (meta-)

362   sedimentary basement rocks south of each set of top-SSW thrust surfaces, the 20–60 kilometers

363   wide, upwards-thickening, wedge-shaped packages are interpreted as crustal-scale, several

364   kilometers thick, north- to NNE-dipping, top-SSW, brittle–ductile thrust systems (see fault zones

365   with high concentration of black lines in Figure 3a–f). These thrust systems include low-angle,

366   brittle–ductile, mylonitic thrust surfaces (black lines in Figure 4d–e) separating upwards-

367   thickening thrust sheets that consist of gently to strongly folded basement rocks and forward-

368   dipping duplex structures (yellow lines in Figure 4d–e). These thrust sheets are interpreted to reflect

369   accretion and stacking from the north or north-northeast. The interpreted thrust systems are

370   comparable in seismic facies and thickness to kilometer-thick mylonitic shear zones in the

371 Norwegian North Sea (Phillips et al. 2016) and southwestern Norwegian Barents Sea (Koehl et al.,

372 2018).

373 N–S-trending folds

374 On E–W seismic cross sections, reflections of the Kongsfjorden–Cowanodden,

375 Bellsundbanken, and Kinnhøgda–Daudbjørnpynten fault zones define large, 50–100 kilometers

376 wide, U-shaped, symmetrical depressions (black lines in Figure 3b) on the edge of which they are

377 truncated at a high angle and overlain by folded lower Paleozoic and mildly folded to flat-lying

378 upper Paleozoic (meta-) sedimentary rocks (purple and orange units with associated yellow lines

379 in Figure 3b). In addition, within these U-shaped depressions, the thrust systems show curving up

380 and down, symmetrical geometries with 5–15 kilometers wavelength (yellow lines within the pink

381 unit in Figure 3b and Figure 4f). Also notice the kilometer- to hundreds of meter-scale undulating

382 pattern of 5–15 kilometers wide curved geometries (yellow lines in Figure 4f). Based on the

383 truncation and abrupt upward disappearance of high-amplitude seismic reflections characterizing

384 the thrust systems, the high-angle truncation of the thrusts is interpreted as a major erosional

385 unconformity (dark blue line in Figure 3b and pink line in Figure 4f), and the large U-shaped

386 depressions as large N–S- to NNE–SSW-trending, upright regional folds (black lines in Figure 3b).

387 Furthermore, the 5–15 kilometers wide, symmetrical, curved geometries and associated, kilometer-

388 to hundreds of meter-scale, undulating pattern of seismic reflections within the thrusts are

389 interpreted as similarly (N–S- to NNE–SSW-) trending, upright, parasitic macro- to meso-scale

390 folds (yellow lines in Figure 3b and Figure 4f).

391 Shallow brittle faults

392 In places, near the top of the 20–60 kilometers wide thrust systems (Kongsfjorden–

393 Cowanodden, Bellsundbanken, and Kinnhøgda–Daudbjørnpynten fault zones), low-angle brittle–

394 ductile thrust surfaces merge upwards with high-angle to vertical, listric, north- to NNE-dipping

395 disruption surfaces at depths of c. 2–3 seconds (TWT; see red lines in Figure 3a and d). These

396 listric disruption surfaces truncate shallow, laterally continuous reflections that display gently

397 curved, symmetric geometries in Storfjorden (yellow lines in Figure 3a) and flat-lying geometries

398 in the northeastern Norwegian Barents Sea (yellow lines in Figure 3d). Notably, they show minor,

399 down-NNE normal offsets, and related minor southwards thickening (towards the disruption) of

400 seismic sub-units within Devonian–Carboniferous (–Permian?) sedimentary strata in the north,

401 both in Storfjorden and the northeastern Barents Sea (Figure 3a–d and white double arrows in

Figure 4g). In addition, they display minor reverse offsets and associated gentle upright folding of shallow continuous reflections potentially representing upper Mesozoic (–Cenozoic?) sedimentary deposits in Storfjorden (Figure 3a–c and e, and orange lines in Figure 4h). Note that flat-lying Mesozoic (–Cenozoic?) sedimentary rocks are not offset in the northeastern Norwegian Barents Sea (Figure 3d).

Based on the observed normal offsets and southwards-thickening of Devonian– Carboniferous (–Permian?) sedimentary strata north of these disruption surfaces (e.g., white double arrows in Figure 4g), these are interpreted as syn-sedimentary Devonian–Carboniferous normal faults. The minor reverse offsets and associated gentle upright folding of Mesozoic (–Cenozoic?) sedimentary rocks in Storfjorden (e.g., orange lines in Figure 4h) suggest that these normal faults were mildly inverted near Svalbard in the Cenozoic. However, it is unclear whether inversion in Storfjorden initiated in the early Cenozoic or later. Nonetheless, minor reverse offset and folding of the seafloor clearly indicate ongoing inversion along these faults (Figure 3a and c, and Figure 4h). Furthermore, considering the merging relationship between these high-angle listric disruption surfaces and underlying shear zones (i.e., merging black and red lines in Figure 3a and c–d), we propose that the formation of Devonian–Carboniferous normal faults was controlled by the crustal-scale, north- to NNE-dipping (inherited) thrust systems (Kongsfjorden–Cowanodden, Bellsundbanken, and Kinnhøgda–Daudbjørnpynten fault zones).

Nordmannsfonna–Sassenfjorden (eastern–central Spitsbergen)

Deep thrust system and N–S-trending folds

Seismic data from Nordmannsfonna to Sassenfjorden in eastern Spitsbergen (see Figure 1c for location) show reflection packages including both planar, continuous, moderately-dipping high-amplitude reflections and upwards-curving, moderate-amplitude reflections (black and yellow lines in Figure 3e–f). These two sets are similar to reflection packages interpreted as low-angle, brittle–ductile mylonitic thrusts bounding packages of south- to SSW-verging folds in Storfjorden and the northeastern Norwegian Barents Sea (black and yellow lines in Figure 3a and d, and supplement S2a). In addition, they are located at similar depths (> 2 seconds TWT) and seem to align with the Kongsfjorden–Cowanodden fault zone in Storfjorden along a WNW–ESE-trending axis. Hence, we interpret the deep, continuous, high-amplitude reflections in eastern Spitsbergen as the western continuation of the top-SSW Kongsfjorden–Cowanodden fault zone. This thrust can

433 be traced on seismic data as gently NNE-dipping, high-amplitude reflections in Sassendalen and

434 Sassenfjorden–Tempelfjorden (supplement S2c–d), and possibly in Billefjorden (Koehl et al., 2021

435 in review, their figure 9a–b).

436   In Nordmannsfonna, the base-Pennsylvanian unconformity (white line in Figure 3e–f; tied

437 to onshore geological maps; Dallmann, 2015) truncates the Kongsfjorden–Cowanodden fault zone

438 (black lines in Figure 3e–f) upwards and the fault shows pronounced variations in dip direction,

439 ranging from east-dipping in the east to NNE-dipping in the north and WNW-dipping in the west,

440 which result into a c. 15–20 kilometers wide, north- to NNE-plunging dome-shaped/convex-

441 upwards geometry (black lines in Figure 3e–f). This portion of the thrust system is interpreted to

442 be folded into a major NNE- to north-plunging upright fold, whose 3D geometry was accurately

443 constrained due to good seismic coverage in this area (Figure 1c).

444   Small-scale structures within the Kongsfjorden–Cowanodden fault zone also show

445 asymmetric folds and internal seismic units terminating upwards with convex-upwards reflections

446 (yellow lines in Figure 3e–f) suggesting top-SSW nappe thrusting in the northern portion of the

447 thrust system. However, on E–W cross sections, seismic data reveal a set of west-verging folds in

448 the east and a more chaotic pattern of symmetrical, dominantly upright folds in the west (yellow

449 lines in Figure 3e) and below a major, high-angle, east-dipping disruption surface (thick red line in

450 Figure 3e) that crosscuts the Kongsfjorden–Cowanodden fault zone.

451 Shallow brittle faults

452   The high-angle, east-dipping disruption surface (thick red line in Figure 3e) is associated

453 with minor subvertical to steeply east-dipping disruption surfaces (thin red lines in Figure 3e). This

454 feature shows a major reverse, top-west offset (> 0.5 second TWT) of seismic units and reflections

455 at depth > 0.75 second (TWT; e.g., black lines in Figure 3e), and minor reverse offset (< 0.1 second

456 TWT) and upwards-convex curving of adjacent reflections at depth < 0.75 second (TWT; white

457 line and yellow lines within blue and units in Figure 3e). Since the major disruption coincides with

458 the location of the Agardhbukta Fault (Piepjohn et al., 2019; see Figure 1 for location) and shows

459 a steep inclination near the surface similar to that of the Agardhbukta Fault, it is interpreted as the

460 subsurface expression of this fault. The Agardhbukta Fault offsets the Kongsfjorden–Cowanodden

461 fault zone in a reverse fashion (>0.5 second TWT; black lines in Figure 3e), and terminates upwards

462 within and slightly offsets upper Paleozoic–Mesozoic sedimentary rocks (blue and black units and

463 associated yellow lines in Figure 3e), which were correlated to onshore outcrops in eastern

464   Spitsbergen (Andresen et al., 1992; Haremo and Andresen, 1992; Dallmann, 2015). As a result,

465   these rocks are folded into a N–S-trending, open, upright fold around the fault tip, both of which

466   suggest top-west movements along the fault (Figure 3e).

467   Pre-Pennsylvanian dykes

468   In the hanging wall and on the eastern flank of the folded Kongsfjorden–Cowanodden fault

469   zone in Nordmannsfonna, high- to low-amplitude, gently east-dipping seismic reflections, which

470   possibly represent sedimentary strata (light orange unit in Figure 3e), are crosscut but not offset by

471   moderately west-dipping, high-amplitude planar reflections (blue lines in Figure 3e). In NNE–

472   SSW-trending cross-sections, these high-amplitude, cross-cutting seismic reflections appear sub-

473   horizontal (blue lines in Figure 3f). These crosscutting, west-dipping reflections are mildly folded

474   in places and either terminate upwards within the suggested, gently east-dipping, sedimentary strata

475   (light orange unit in Figure 3e) or are truncated by the base-Pennsylvanian unconformity (white

476   line in Figure 3e). Downwards within the Kongsfjorden–Cowanodden fault zone (black lines in

477   Figure 3e), these inclined reflections can be vaguely traced as a series of discontinuous, subtle

478   features (see blue lines in Figure 3e). In the footwall of the Kongsfjorden–Cowanodden fault zone,

479   the inclined reflections become more prominent again, still do not offset background reflections,

480   and extend to depths of 3–3.5 seconds (TWT; blue lines in Figure 3e). The high amplitude of these

481   planar west-dipping reflections, the absence of offset across them, and their discontinuous

482   geometries across the Agardhbukta Fault and the Kongsfjorden–Cowanodden fault zone suggest

483   that they may represent dykes (see Phillips et al., 2018). Because they appear truncated by the Base-

484   Pennsylvanian unconformity, we suggest such dykes were emplaced prior to development of this

485   unconformity. The Kongsfjorden–Cowanodden fault zone is folded into a broad, 15–20 kilometers

486   wide anticline, and offset > 0.5 second (TWT) by the Agardhbukta Fault, whereas the west-dipping

487   dykes (blue lines in Figure 3e) and the gently east-dipping sedimentary strata they intrude (light

488   orange unit in Figure 3e) are only mildly folded and show no offset across the Agardhbukta Fault

489   (Figure 3e). These differences in deformation suggest that the latter were deformed during a mild

490   episode of late contraction but not by the same early episode of intense contraction that resulted in

491   macrofolding of the Kongsfjorden–Cowanodden fault zone.

492   Cretaceous dykes and sills

493   Near or at the surface, thin, kilometer-wide, lenticular packages of gently dipping,

494   moderate–high-amplitude seismic reflections (black units in Figure 3e–f) correlate with surface

495   outcrops of Cretaceous sills of the Diabasodden Suite in eastern Spitsbergen (Senger et al., 2013;

496   Dallmann, 2015). In places, these sills are associated with areas showing high-frequency

497   disruptions of underlying sub-horizontal seismic reflections (dotted black lines in Figure 3f)

498   correlated with onshore occurrences of Pennsylvanian–Mesozoic sedimentary strata (Andresen et

499   al., 1992; Haremo and Andresen, 1992; Dallmann, 2015). We interpret these areas of high-

500   frequency disruption in otherwise relatively undisturbed and only mildly deformed Pennsylvanian–

501   Mesozoic sedimentary strata as zones with occurrences of Cretaceous feeder dykes. Alternatively,

502   disruption may be related to scattering and attenuation of seismic energy caused on the sills.

503

504   *Stappen High (northwestern Norwegian Barents Sea north of Bjørnøya)*

505   On the Stappen High between Bjørnøya and Spitsbergen (Figure 1c), seismic reflections at

506   depth of 2–6 seconds (TWT) are dominated by moderate- to high-amplitude reflections with

507   limited (< five kilometers) lateral continuity showing asymmetric, dominantly SSW-leaning

508   curving geometries with a few hundreds of meters to a few kilometers width (yellow lines within

509   pink unit in Figure 3c), i.e., analogous to those in folded Precambrian basement rocks farther north

510   (Figure 3a and Figure 4a). These reflections are truncated by gently to moderately NNE- (and

511   subsidiary SSW-) dipping disruption surfaces (black lines within pink and purple units in Figure

512   3c), some of which connect upwards with shallow (0–2 seconds TWT), NNE-dipping, high-angle

513   listric disruptions near Bjørnøya in the south (red lines in Figure 3c). Notably, major seismic

514   reflections near the upwards termination of deep, moderately–gently NNE-dipping disruption

515   surfaces display characteristic gently curving-upwards geometries (yellow lines within pink and

516   purple units in Figure 3c) and overlying seismic onlaps (white half arrows in Figure 3c) similar to

517   those observed just south of major NNE-dipping thrust systems in Storfjorden and the northeastern

518   Norwegian Barents Sea (Figure 3a and supplement S2).

519   We interpret deep (2–6 seconds TWT), curving, discontinuous seismic reflections ((yellow

520   lines within pink and purple units in Figure 3c) as folded Precambrian–lower Paleozoic basement

521   rocks, and dominantly NNE-dipping disruption surfaces (black lines within pink and purple units

522   in Figure 3) as brittle–ductile thrust possibly partly mylonitic, though with less intense deformation

523   than the major NNE-dipping thrust systems observed farther north in Storfjorden and the

524   northeastern Norwegian Barents Sea, like the Kongsfjorden–Cowanodden fault zone. These

525   brittle–ductile thrusts can be traced eastwards on seismic data on the Stappen High and into the

526   Sørkapp Basin (Figure 1c).

527   Based on their geometries and on gentle folding of the seafloor reflection (yellow lines

528   within green unit in Figure 3c), shallow, NNE-dipping, high-angle listric disruptions are interpreted

529   as mildly inverted normal faults overprinting deep NNE-dipping thrusts. Based on previous

530   fieldwork on Bjørnøya (Worsley et al., 2001), on seismic mapping in the area (Lasabuda et al.,

531   2018), and on well tie to Hopen and Edgeøya, relatively continuous (> five kilometers) shallow

532   (0–2 seconds TWT), gently curved–undulating seismic reflections overlying folded Precambrian–

533   lower Paleozoic basement rocks are interpreted as mildly folded upper Paleozoic–Mesozoic (–

534   Cenozoic?) sedimentary strata (orange and green units in Figure 3c).

535

Potential field data and regional gravimetric and magnetic anomalies
536

NNE-dipping thrusts
537

538   In the northern Barents Sea, Storfjorden and central–eastern Spitsbergen, the seismic

539   occurrences   of   the   Kongsfjorden–Cowanodden,   Bellsundbanken   and   Kinnhøgda–

540   Daudbjørnpynten fault zones coincide with gradual, step-like, southwards increases in gravimetry

541   and, in places, with high magnetic anomalies in cross-section (Figure 3a–b and d–f). Similar

542   southwards gradual and step-like increases in the Bouguer and magnetic anomalies correlate with

543   major thrusts north of Bjørnøya (Figure 3c; see Figure 1b for location of Bjørnøya). These patterns

544   suggest that the footwall of the thrust systems consists of relatively denser rock units, possibly with

545   higher metamorphic grade. Seismic interpretation showing thickening of metamorphosed and

546   folded Precambrian basement rock units (pink unit in Figure 3a and c–d) in the footwall of the

547   thrusts further support this claim.

548   In map-view gravimetric and magnetic data, the three thrust systems in Storfjorden (black

549   lines in Figure 3a) coincide with three high, WNW–ESE-trending, continuous, gently undulating

550   (and, in place, merging/splaying) gravimetric and discontinuous magnetic anomalies (dashed

551   yellow lines in Figure 5a–c) that are separated from each other by areas showing relatively low

552   gravimetric and magnetic anomalies (e.g., see green to blue areas in Figure 5a). Some of these

553   anomalies extend from central Spitsbergen to Storfjorden and the northern Barents Sea (below the

554   Ora and Olga basins) as curving, E–W- and NW–SE-trending, 50–100 kilometers wide anomalies

555   (dashed yellow lines in Figure 5a–c). Analogously, thrust systems north of Bjørnøya (Figure 3c)

and north of the Ora and Olga basins (supplement S2b) correlate with comparable WNW–ESE-trending, curving magnetic and gravimetric anomalies (dashed yellow lines in Figure 5a–c). The WNW–ESE-trending anomalies appear clearer by using a slope-direction shader for gravimetric data, which accentuates the contrast between each trend of anomalies (green and red areas in Figure 5b).

Most of the recognized, regional WNW–ESE-trending magnetic and gravimetric anomalies (dashed yellow lines in Figure 5a–c) can be traced into the Russian Barents Sea where they are linear and are crosscut by major N–S- to NNW–SSE-trending anomalies (dashed black and white lines in Figure 5a–c). Subtle WNW–ESE-trending magnetic and gravimetric anomalies further extend onshore northwestern Russia (e.g., Kanin Peninsula and southern Novaya Zemlya) where they correlate with major Timanian thrusts and folds, some of which are suspected to extend thousands of kilometers between northwestern Russia and the Varanger Peninsula in northern Norway (e.g., Trollfjorden–Komagelva Fault Zone and Central Timan Fault and associated Mikulkin Antiform; Siedlecka, 1975; Siedlecka and Roberts, 1995; Olovyanishnikov et al., 2000; Lorenz et al., 2004; Kostyuchenko et al., 2006). In addition, two of the southernmost WNW–ESE-trending gravimetric and magnetic anomalies coincide with the location of well known, crustal-scale, SSW-verging Timanian thrust faults, the Trollfjorden–Komagelva Fault Zone and the Central Timan Fault. Thus, based on their overall WNW–ESE trend, patterns of alternating highs and lows both for gravimetric and magnetic anomalies (see Figure 5a), location at the boundary of oppositely dipping slopes (see slope-direction shader map in Figure 5b), and extensive field studies and seismic and well data in northwestern Russia (e.g., Kanin Peninsula and Timan Range; Siedlecka and Roberts, 1995; Olovyanishnikov et al., 2000; Lorenz et al., 2004; Kostyuchenko et al., 2006), northern Norway (e.g., Varanger Peninsula; Siedlecka, 1975), and the southeastern Norwegian Barents Sea (Hassaan et al., 2021), WNW–ESE-trending anomalies are interpreted as a combination of basement-seated Timanian macrofolds and top-SSW reverse faults (Figure 5a–c).

N–S-trending folds

Large N–S-trending open folds (e.g., black and yellow lines in Figure 3b) coincide with N–S- to NNE–SSW-trending, 20–100 kilometers wide, arcuate gravimetric and magnetic anomalies (dashed white and black lines in Figure 5a–c), which are highly oblique to WNW–ESE-trending

587   gravimetric and magnetic anomalies and thrust systems (dashed yellow lines in Figure 5a–c).

588   Notably, major N–S- to NNE–SSW-trending synclines in Figure 3b (marked as red lines over a

589   white line in Figure 5a and c and as pink lines over a red line in Figure 5b) coincides with similarly

590   trending gravimetric and magnetic anomalies (dashed black lines in Figure 5a and c and dashed

591   white lines in Figure 5b). On the slope-direction shader map of gravimetric data, these N–S- to

592   NNE–SSW-trending anomalies are localized along the boundary between areas with eastwards-

593   (ca. 90–100°; blue areas in Figure 5b) and westwards-facing slopes (ca. 270–280°; white areas in

594   Figure 5b).

595   Notably where the main thrusts are preserved, major N–S-trending synforms (see 50–60

596   kilometers wide U-shaped depression formed by the Kinnhøgda–Daudbjørnpynten fault zone, i.e.,

597   black lines, in Figure 3b) coincide with gravimetric and magnetic highs (white and black dashed

598   lines in Figure 5a–c), whereas major antiforms where major NNE-dipping thrusts are partly eroded

599   (e.g., c. 100 kilometers wide areas where the Kinnhøgda–Daudbjørnpynten fault zone is absent in

600   Figure 3b) coincide with gravimetric and magnetic lows (the lows are parallel to white and black

601   dashed lines symbolizing magnetic and gravimetric highs in Figure 5a–c). The correlation of the

602   interpreted NNE-dipping thrust systems with gravimetric highs suggests that the thrusts consist of

603   relatively denser rocks. This supports the inferred mylonitic (i.e., higher metamorphic grade)

604   component of the thrusts because mylonites are relatively denser due to the formation of high-

605   density minerals with increasing deformation (e.g., Arbaret and Burg, 2003; Colombu et al., 2015).

606   In the northwestern part of the Barents Sea (i.e., area covered by seismic data presented in

607   Figure 3), N–S- to NNE–SSW-trending gravimetric and magnetic anomalies (white and black

608   dashed lines in Figure 5a–c) are typically 20–50 kilometers wide and correlate with similarly

609   trending Caledonian folds and thrusts onshore Nordaustlandet (e.g., Rijpdalen Anticline; Johansson

610   et al., 2004; 2005; Dumais and Brönner, 2020) and northeastern Spitsbergen (e.g., Atomfjella

611   Antiform; Gee et al., 1994; Witt-Nilsson et al., 1998), whose width is comparable to that of the

612   anomalies. In the south, N–S- to NNE–SSW-trending gravimetric and magnetic anomalies merge

613   together and swing into a NE–SW trend onshore–nearshore the Kola Peninsula and northern

614   Norway. These anomalies mimic the attitude of Caledonian thrusts and folds in the southern

615   Norwegian Barents Sea (Gernigon and Brönner, 2012; Gernigon et al., 2014) and onshore northern

616   Norway (Sturt et al., 1978; Townsend, 1987; Roberts and Williams, 2013). In the east, N–S- to

617 NNE–SSW-trending anomalies broaden to up to 150 kilometers in the Russian Barents Sea (Figure

618 5a–c).

619   In places, the intersections of high, WNW–ESE- and N–S- to NNE–SSW-trending

620 gravimetric and magnetic anomalies generate relatively higher, oval-shaped anomalies (e.g., dotted

621 white lines in Figure 5a and c). Notable examples are found in the Ora and Olga basins and east

622 and south of these basins (see dotted white lines in Figure 5a and c).

623

624 **Discussion**

625   In the discussion, we consider the lateral extent of the interpreted NNE-dipping thrust

626 systems, their possible timing of formation, and potential episodes of reactivation and overprinting.

627 Then we briefly discuss the implications of these thrust systems for plate tectonics reconstructions

628 in the Arctic.

629

630 *Extent of NNE-dipping thrust systems*

631   Four major NNE-dipping systems of mylonitic thrusts and shear zones (Steiløya–Krylen,

632 Kongsfjorden–Cowanodden, Bellsundbanken, Kinnhøgda–Daudbjørnpynten fault zones) were

633 identified at depths > 1–2 seconds (TWT) in central–eastern Spitsbergen, Storfjorden and the

634 northeastern Barents Sea, and several systems with less developed ductile fabrics between

635 Spitsbergen and Bjørnøya on the Stappen High (Figure 3a–f).

636   The Kongsfjorden–Cowanodden fault zone is relatively easy to trace and correlate in

637 Sassenfjorden, Sassendalen, Nordmannsfonna, Storfjorden and the northeastern Barents Sea (east

638 of Edgeøya) because (i) the seismic data in the these areas have a high resolution and good

639 coverage, (ii) internal seismic reflections are characterized by high amplitudes (e.g., brittle–ductile

640 thrusts and mylonitic shear zones), (iii) kinematic indicators within the thrust system consistently

641 show dominantly top-SSW sense of shear with SSW-verging fold structures (Figure 3a and d–f,

642 and supplement S2), (iv) the geometry and kinematics indicators along shallow brittle overprints

643 are regionally consistent (listric, down-NNE, brittle normal faults; Figure 3a and d–f), and (v) this

644 thrust consistently coincides with increase in gravimetric and magnetic anomaly in cross-section

645 (Figure 3a and d) and with analogously trending gravimetric and magnetic anomalies in central–

646 eastern Spitsbergen and the northern Barents Sea (Figure 5a–b). This thrust system was previously

647 identified below the Ora Basin by Klitzke et al. (2019), though interpreted as potential Timanian

648   grain instead of a discrete structure. The proposed correlation based on seismic, and cross-section

649   and map-view gravimetric and magnetic data suggests a lateral extent of c. 550–600 kilometers

650   along strike for the Kongsfjorden–Cowanodden fault zone. However, the regional magnetic and

651   gravimetric anomalies associated with this thrust in the Norwegian Barents Sea and Svalbard

652   extend potentially farther east as a series of WNW–ESE-trending anomalies to the mainland of

653   Russia (Figure 5a–c). Notably, these anomalies correlate with the southern edge of Novaya Zemlya

654   (Figure 5a–c) and, more specifically, with WNW–ESE-striking fault segments of the Baidaratsky

655   fault zone (Figure 1a; Lopatin et al., 2001; Korago et al., 2004), a major thrust fault that bounds a

656   major basement high in the central Russian Barents Sea, the Ludlov Saddle (Johansen et al., 1992;

657   Drachev et al., 2010). Thus, it is possible that the Kongsfjorden–Cowanodden fault zone also

658   extends farther east, possibly merging with the Baidaratsky fault zone, i.e., with a minimum extent

659   of 1700–1800 kilometers (Figure 5a–c). This is supported by a similar configuration of the

660   Baidaratsky Fault Zone and the Kongsfjorden–Cowanodden fault zone, including a basement-

661   seated, low-angle thrust geometry of both faults and inversion as a normal fault and deposition of

662   several seconds (TWT) thick sedimentary strata in the hanging wall of the faults in the late

663   Paleozoic (Figure 3d and Smelror et al., 2009 their profile C–D pp. 53).

664   The overall NNE-dipping and folded (into NNE-plunging folds) geometry of the

665   Kongsfjorden–Cowanodden fault zone (Figure 3e–f and Klitzke et al., 2019, their figures 3–5) may

666   explain the alternating NW–SE- and E–W-trending geometry of the gravimetric and magnetic

667   anomalies correlating with this thrust system (Figure 5a–b). E–W- and NW–SE-trending segments

668   of these anomalies may represent respectively the western and eastern limbs of open, gently NNE-

669   plunging macro-anticlines in the northern Norwegian Barents Sea. The relatively higher, oval-

670   shaped gravimetric and magnetic anomalies at the intersection of WNW–ESE- and N–S- to NNE–

671   SSW-trending magnetic and gravimetric highs, which are interpreted as the interaction of two sub-

672   orthogonal fold trends further support this claim (Figure 5a and c).

673   Interpretation of seismic sections (Figure 3e–f and supplement S2) and regional magnetic

674   and gravimetric data (Figure 5a–c) in central–eastern Spitsbergen show that NNE-dipping, top-

675   SSW Kongsfjorden–Cowanodden and Bellsundbanken fault zones likely extend westwards into

676   central (and possibly northwestern) Spitsbergen (e.g., Sassendalen, Sassenfjorden, Tempelfjorden,

677   and Billefjorden; see Figure 1c for locations). This is further supported by recent field, bathymetric

678   and seismic mapping in central Spitsbergen showing that (inverted) Devonian–Carboniferous

NNE-dipping brittle normal faults in Billefjorden and Sassenfjorden–Tempelfjorden merge with kilometer-scale, NNE-dipping, Precambrian basement fabrics and shear zones at depth (Koehl, 2020a; Koehl et al., 2021 in review). Other examples of WNW–ESE-trending fabrics include faults within Precambrian basement and Carboniferous sedimentary rocks in northeastern Spitsbergen (Witt-Nilsson et al., 1998; Koehl and Muñoz-Barrera, 2018), and within Devonian sedimentary rocks in northern and northwestern Spitsbergen (Friend et al., 1997; McCann, 2000; Dallmann and Piepjohn, 2020). These suggest a repeated and regional influence of WNW–ESE-trending thrust systems and associated basement fabrics in Spitsbergen.

Analogously to the Kongsfjorden–Cowanodden fault zone, the Bellsundbanken and Kinnhøgda–Daudbjørnpynten fault zones (Figure 3a) geometries and kinematics on seismic data, and their coinciding with parallel gravimetric and magnetic anomalies in map view and with magnetic and gravimetric highs in cross-section suggest that they extend from Storfjorden to the island of Hopen (Figure 1c, Figure 3a, Figure 5a–c, and supplement S2). Notably, a 50–100 kilometers wide, NNE–SSW-trending gravimetric and associated magnetic anomaly interpreted as Caledonian grain in Nordaustlandet (Rijpdalen Anticline; Dumais and Brönner, 2020) bends across the trace of these two thrust systems (Figure 5a–c). Farther east, the Bellsundbanken and Kinnhøgda–Daudbjørnpynten fault zones parallel gravimetric and magnetic, alternating E–W- and NW–SE-trending anomalies that follow the trends and map-view shapes of the Ora and Olga basins in the northeastern Norwegian Barents Sea (Anell et al., 2016; see Figure 1b–c for location). This suggests that these two thrust systems extend into the northeastern Norwegian Barents Sea and, potentially, into the Russian Barents Sea, and affected the development of Paleozoic sedimentary basins. This is also the case of the Steiløya–Krylen fault zone (supplement S2b), which coincides with mild, discontinuous, WNW–ESE-trending gravimetric and magnetic anomalies that extend well into the Russian Barents Sea and, possibly, across Novaya Zemlya (Figure 5a–c).

In southwestern Spitsbergen, field mapping revealed the presence of a major, subvertical, kilometer-thick, WNW–ESE-striking mylonitic shear zone metamorphosed under amphibolite facies conditions, the Vimsodden–Kosibapasset Shear Zone (Majka et al., 2008, 2012; Mazur et al., 2009; see Figure 1c for location). This major sinistral shear zone aligns along a WNW–ESE-trending axis with the Kinnhøgda–Daudbjørnpynten fault zone in the northwestern Norwegian Barents Sea (Figure 3a), and shows a folded geometry in map view that is comparable to that of major NNE-dipping thrust systems in the northern Norwegian Barents Sea (Figure 3a and e–f,

Figure 5a–c, and supplement S2; Klitzke et al., 2019). In addition, the Vimsodden–Kosibapasset Shear Zone juxtaposes relatively old Proterozoic basement rocks in the north against relatively young rocks in the south, thus suggesting a similar configuration and kinematics as along the Kinnhøgda–Daudbjørnpynten fault zone in Storfjorden and the northeastern Norwegian Barents Sea. Moreover, von Gosen and Piepjohn (2001) and Bergh and Grogan (2003) reported that Devonian–Mississippian sedimentary successions and Cenozoic fold structures (e.g., Hyrnefjellet Anticline) are offset sinistrally by a few kilometers in Hornsund. Thus, we propose that the Vimsodden–Kosibapasset Shear Zone extends into Hornsund and represents the westwards continuation of the Kinnhøgda–Daudbjørnpynten fault zone. This suggests a minimum extent of 400–450 kilometers for this thrust system (Figure 1b–c and Figure 5a–c).

Timing of formation of major NNE-dipping thrust systems and N–S-trending folds

NNE-dipping thrust systems

The several-kilometer thickness and hundreds–thousands of kilometers along-strike extent of NNE-dipping thrust systems in central–eastern Spitsbergen, Storfjorden, and the northwestern and northeastern Norwegian Barents Sea suggest that they formed during a major contractional tectonic event. The overall WNW–ESE trend and the consistent north-northeastwards dip and top-SSW sense of shear along the newly evidenced deep thrust systems preclude formation during the Grenvillian, Caledonian, and Ellesmerian orogenies, and the Eurekan tectonic event. These tectonic events all involved dominantly E–W-oriented contraction and resulted in the formation of overall N–S- to NNE–SSW-trending fabrics, structures and deformation belts in Svalbard (i.e., sub-orthogonal to the newly identified thrust systems) such as the Atomfjella Antiform (Gee et al., 1994; Witt-Nilsson et al., 1998), the Vestfonna and Rijpdalen anticlines (Johansson et al., 2004; 2005; Dumais and Brönner, 2020), the Dickson Land and Germaniahalvøya fold-thrust zones (McCann, 2000; Piepjohn, 2000; Dallmann and Piepjohn, 2020), and the West Spitsbergen Fold-and-Thrust Belt and related early Cenozoic structures in eastern Spitsbergen (Andresen et al., 1992; Haremo and Andresen, 1992; Dallmann et al., 1993), and NE–SW- to NNE–SSW-striking thrusts and folds in northern Norway (Sturt et al., 1978; Townsend, 1987; Roberts and Williams, 2013) and the southwestern Barents Sea (Gernigon et al., 2014).

A possible cause for the formation of the observed NNE-dipping thrust systems is the late Neoproterozoic Timanian Orogeny, which is well known onshore northwestern Russia (e.g., Kanin

Peninsula, Timan Range and central Timan; Siedlecka and Roberts, 1995; Olovyanishnikov et al., 2000; Lorenz et al., 2004; Kostyuchenko et al., 2006) and northeastern Norway (Varanger Peninsula; Siedlecka and Siedlecki, 1967; Siedlecka, 1975; Roberts and Olovyanishnikov, 2004), and traces of which were recently found in the southeastern Norwegian Barents Sea (Hassaan et al., 2020a, 2020b, 2021; Hassaan, 2021), in southwestern Spitsbergen (Majka et al., 2008, 2012, 2014) and northern Greenland (Rosa et al., 2016; Estrada et al., 2018). The overall transport direction during this orogeny was directed towards the south-southwest and most thrust systems show NNE-dipping geometries (Olovyanishnikov et al., 2000; Lorenz et al., 2004; Kostyuchenko et al., 2006), e.g., the Timanian thrust front on the Varanger Peninsula in northeastern Norway (Trollfjorden–Komagelva Fault Zone; Siedlecka and Siedlecki, 1967; Siedlecka, 1975) and its eastwards continuation, the Central Timan Fault (Lorenz et al., 2004; Kostyuchenko et al., 2006). In addition, the size of Timanian thrust systems and related thrust anticlines in the Timan Range and Kanin Peninsula (e.g., Central Timan Fault and Mikulkin Antiform) are comparable ($\geq$ 3–4 seconds TWT thick thrusts and 5–15 kilometers wide thrust-related major anticlines; Lorenz et al., 2004 their figures 3 and 5; Kostyuchenko et al., 2006 their figure 17) to that of thrust and fold systems in the northern Norwegian Barents Sea and Svalbard (Figure 3a and c–d).

Thus, based on their overall WNW–ESE strike (Figure 1b–c), their vergence to the south-southwest (Figure 3a, c–d and f), their coincidence with gravimetric and magnetic highs (Figure 5a–c), their upward truncation by a major unconformity consistently throughout the study area (see top-Precambrian unconformity in Figure 3a–d), and the correlation of these NNE-dipping thrusts and associated major anticlines (via gravimetric and magnetic anomalies) to similarly striking and verging structures of comparable size (i.e., several seconds TWT thick, 5–15 kilometers wide anticlines) onshore–nearshore northwestern Russia and northern Norway (Siedlecka, 1975; Siedlecka and Roberts, 1995; Olovyanishnikov et al., 2000; Roberts and Siedlecka, 2002; Lorenz et al., 2004; Gee and Pease, 2004; Kostyuchenko et al., 2006), NNE-dipping thrusts in the northern Norwegian Barents Sea, Storfjorden, and central–eastern Spitsbergen are interpreted as the western continuation of Timanian thrust and fold systems.

Timanian grain was recently identified in the northeastern Norwegian Barents Sea through interpretation of new seismic, magnetic and gravimetric datasets shown in Figure 5a–c (Klitzke et al., 2019). The alignment, coincident location, and matching geometries (e.g., curving E–W to NW–SE strike/trend and kilometer-wide NNE–SSW-trending anticline) between Timanian grain

772 and structures mapped by Klitzke et al. (2019) and the major, NNE-dipping, top-SSW thrust
773 systems described in central–eastern Spitsbergen, Storfjorden and the Norwegian Barents Sea
774 (Figure 3a–f and supplement S2) further support a Timanian origin for the latter. Further evidence
775 of relic Timanian structural grain as far as the Loppa High and Bjørnøya Basin are documented by
776 previous magnetic studies and modelling (Marello et al., 2010). Moreover, seismic mapping
777 suggests that Timanian thrust systems extend well into central Spitsbergen (Figure 3e–f and
778 supplement S2c–d; Koehl, 2020a; Koehl et al., 2021 in review), and regional gravimetric and
779 magnetic anomaly maps suggest that Timanian thrust systems might extend farther west to (north-
780) western Spitsbergen (Figure 5a–c).

781 Probable reasons as to why these major (hundreds–thousands of kilometers long) thrust
782 systems were not identified before during fieldwork in Svalbard are their burial to high depth (>
783 1–2 seconds TWT in the study area, i.e., several kilometers below the surface; Figure 3a–f), and
784 their strong overprinting by younger tectonic events like the Caledonian Orogeny in areas where
785 they are exposed (e.g., Vimsodden–Kosibapasset Shear Zone in southwestern Spitsbergen;
786 Faehnrich et al., 2020). Possible areas of interest for future studies include the western and
787 northwestern parts of Spitsbergen where Caledonian and Eurekan E–W contraction contributed to
788 uplift and exhume deep basement rocks, and where Timanian rocks potentially crop out (e.g.,
789 Peucat et al., 1989).

790

791 *N–S-trending folds*

792 N–S-trending upright folds involve the NNE-dipping thrust systems (Figure 3b and e) and
793 correlate (via gravimetric and magnetic anomalies) with major Caledonian folds in northeastern
794 Spitsbergen and Nordaustlandet, like the Atomfjella Antiform (Gee et al., 1994; Witt-Nilsson et
795 al., 1998) and Rijpdalen Anticline (Johansson et al., 2004; 2005; Dumais and Brönner, 2020), with
796 Caledonian grain in the southern Norwegian Barents Sea (Gernigon and Brönner, 2012; Gernigon
797 et al., 2014), and with major NE–SW-trending Caledonian folds onshore northern Norway (Sturt
798 et al., 1978; Townsend, 1987; Roberts and Williams, 2013). In addition, the width of the NE–SW-
799 to N–S-trending gravimetric and magnetic anomalies associated with these folds increases up to
800 150 kilometers eastwards, i.e., away from the Caledonian collision zone (Figure 5a–c; Corfu et al.,
801 2014; Gasser, 2014). Thus, N–S-trending folds in the northern Norwegian Barents Sea are
802 interpreted as Caledonian regional folds in Precambrian–lower Paleozoic rocks. The relatively

broader geometry of Caledonian folds away from the Caledonian collision zone (e.g., in the Russian Barents Sea) is inferred to be related to gentler fold geometries due to decreasing deformation intensity in this direction. This is further supported by relatively low grade Caledonian metamorphism in Franz Josef Land (Knudsen et al., 2019; see Figure 1a–b for location). By contrast, the presence of tighter Caledonian folds near the collision zone in the northern Norwegian Barents Sea (e.g., Figure 3b and e, and Atomfjella Antiform and Rijpdalen Anticline onshore; Gee et al., 1994; Witt-Nilsson et al., 1998; Johansson et al., 2004, 2005; Dumais and Brönner, 2020) is associated with much narrower (20–50 kilometers wide) gravimetric and magnetic anomalies (Figure 5a–c). Note that the Atomfjella Antiform and Rijpdalen Anticline can be directly correlated with 20–50 kilometers wide, N–S-trending high gravimetric and magnetic anomalies (Figure 5a–c). Noteworthy, some of the NNE–SSW-trending folds and anomalies in the northernmost Norwegian Barents Sea may reflect a combination of Caledonian and superimposed early Cenozoic Eurekan folding (e.g., Kairanov et al., 2018).

The interference of WNW–ESE- and N–S- to NNE–SSW-trending gravimetric highs, which are correlated to Timanian and Caledonian folds respectively, produces oval-shaped gravimetric and magnetic highs (Figure 5a). These relatively higher, oval-shaped gravimetric anomalies are interpreted to correspond to dome-shaped folds resulting from the interaction of Timanian and Caledonian folds involving refolding of WNW–ESE-trending Timanian folds during E–W Caledonian contraction. Field studies on the Varanger Peninsula in northern Norway and seismic studies of Timanian thrusts off northern Norway where the interaction of Timanian and Caledonian folds produced dome-shaped fold structures (Ramsay, 1962), e.g., like the Ragnarokk Anticline (Siedlecka and Siedlecki, 1971; Koehl, in prep.) also support this interpretation. Furthermore, Barrère et al. (2011) suggested that basins and faults in the southern Norwegian Barents Sea are controlled by the interaction of Caledonian and Timanian structural grain, and Marello et al. (2010) argued that elbow-shaped magnetic anomalies reflect the interaction of Caledonian and Timanian structural grains in the Barents Sea, potentially as far west as the Loppa High and the Bjørnøya Basin.

Phanerozoic reactivation and overprinting of Timanian thrust systems
Caledonian reactivation and overprint

The geometry of the Kongsfjorden–Cowanodden and Kinnhøgda–Daudbjørnpynten fault zones in Nordmannsfonna (Figure 3e) and in the northeastern Norwegian Barents Sea (Figure 3b; Klitzke et a., 2019), where they are folded into broad NNE-plunging upright anticlines and synclines suggests that these thrust systems were deformed after they accommodated top-SSW Timanian thrusting (Figure 6a and Figure 7a). In addition, subsidiary top-west kinematics (west-verging folds and top-west minor thrusts) suggest that Timanian thrust systems were partly reactivated–overprinted during an episode of intense E–W contraction (Figure 6b and Figure 7b). However, west-dipping dykes crosscutting and gently east-dipping sedimentary strata overlying the eastern part of the folded Kongsfjorden–Cowanodden fault zone are only mildly folded, and upper Paleozoic sedimentary strata lie flat over folded and partly eroded Precambrian–lower Paleozoic rocks and the Kinnhøgda–Daudbjørnpynten fault zone, thus suggesting that these sedimentary strata and dykes were not involved in this episode of E–W contraction (Figure 3e).

A notable episode of E–W contraction in Svalbard is the Caledonian Orogeny in the early–mid Paleozoic, which resulted in the formation of west-verging thrusts and N–S-trending folds of comparable size (c. 15–25 kilometers wide) to those affecting the Kongsfjorden–Cowanodden and Kinnhøgda–Daudbjørnpynten fault zones in Nordmannsfonna and the northern Norwegian Barents Sea (Figure 3b and e; Klitzke et al., 2019, their figures 3–5), such as the Atomfjella Antiform in northeastern Spitsbergen (Gee et al., 1994; Witt-Nilsson et al., 1998; Lyberis and Manby, 1999) and the Rijpdalen Anticline in Nordaustlandet (Figure 1b). Since the NNE-plunging anticline in Nordmannsfonna does not affect overlying Pennsylvanian–Mesozoic sedimentary strata (Figure 3e), we propose that they formed during Caledonian contraction (Figure 7b). This is supported by the involvement of the top-Precambrian unconformity and underlying NNE-dipping thrusts in N–S- to NNE-SSW-trending folds, and by the truncation of these folds by the top-Silurian unconformity, which is onlapped by mildly deformed to flat-lying upper Paleozoic strata (Figure 3b and Figure 4f). Furthermore, structures with geometries comparable to NNE-plunging folds in the northern Barents Sea and Svalbard were observed in northern Norway. An example is the Ragnarokk Anticline, a dome-shaped fold structure along the Timanian front thrust on the Varanger Peninsula, which results from the re-folding of Timanian thrusts and folds into a NE–SW-trending Caledonian trend (Siedlecka and Siedlecki, 1971).

Further support of a Caledonian origin for upright NNE-plunging folds in eastern Spitsbergen, Storfjorden and the northern Norwegian Barents Sea is that these folds are relatively

tight in the west, in Nordmannsfonna and the northwestern Barents Sea (Figure 3b and e), whereas they show gradually gentler and more open geometries in the east, i.e., away from the Caledonian collision zone (Figure 3b). This is also shown by the gradual eastwards broadening of regional gravimetric and magnetic anomalies correlated with Caledonian folds suggesting gentler fold geometries related to decreasing (Caledonian) deformation intensity in this direction (Figure 5a–c). This contrasts with the homogeneous intensity of deformation along NNE-dipping thrusts on seismic data and with the homogeneous width of related gravimetric–magnetic anomalies from west to east in Svalbard and the Barents Sea (Figure 3a–f and Figure 5a–c and supplement S2). Caledonian folding of Timanian thrusts also explains the weaker magnetic and gravimetric signal of Timanian faults at the location of major Caledonian synclines where Timanian faults were transported downwards and, therefore, may not show well on potential field data (e.g., major two, NE–SW- to N–S-trending, negative gravimetric anomalies in the Russian Barents Sea just west of Novaya Zemlya; Figure 5a).

In Nordmannsfonna, the Caledonian origin of the major 15–20 kilometers wide anticline, and the truncation of overlying, gently east-dipping, mildly folded sedimentary strata and crosscutting west-dipping dykes by the base-Pennsylvanian unconformity suggest that these sedimentary strata and dykes are Devonian (–Mississippian?) in age (Figure 6c–d). This is supported by the presence of thick Devonian–Mississippian collapse deposits in adjacent areas of central–northern Spitsbergen (Cutbill et al., 1976; Murascov and Mokin, 1979; Aakvik, 1981; Gjelberg, 1983; Manby and Lyberis, 1992; Friend et al., 1997), and by Middle Devonian to Mississippian ages (395–327 Ma) for dykes in central–northern Spitsbergen (Evdokimov et al., 2006), northern Norway (Lippard and Prestvik, 1997; Guise and Roberts, 2002), and northwestern Russia (Roberts and Onstott, 1995).

The occurrence of a > 0.5 second (TWT) reverse offset of the folded Kongsfjorden–Cowanodden fault zone and the lack of offset of the Devonian (–Mississippian?) dykes across the Agardhbukta Fault indicate that the latter fault formed as a top-west thrust during the Caledonian Orogeny. At depth, the Agardhbukta Fault merges with the eastern flank of the folded Kongsfjorden–Cowanodden fault zone. This, together with the presence of minor, high-angle, top-west brittle thrusts within the Kongsfjorden–Cowanodden fault zone (Figure 3e), indicates that the Agardhbukta Fault reactivated and/or overprinted the eastern portion of the Kongsfjorden–Cowanodden fault zone in Nordmannsfonna during Caledonian contraction (Figure 6b and Figure

895 7b). Depth conversion using seismic velocities from Gernigon et al. (2018) suggest that the
896 Agardhbukta Fault offset the Kongsfjorden–Cowanodden fault zone by ca. 2.4–2.5 kilometers top-
897 west during Caledonian contraction (Figure 3e and supplement S3g). These kinematics are
898 consistent with field observation in eastern Spitsbergen by Piepjohn et al. (2019, their figure 17b).
899 However, Piepjohn et al. (2019) also suggested a significant component of Mesozoic–Cenozoic,
900 down-east normal movement, which was not identified on seismic data in Nordmannsfonna. This
901 suggests either along strike variation in the movement history of the Agardhbukta Fault, either that
902 the fault mapped on seismic data in Nordmannsfonna does not correspond to the Agardhbukta Fault
903 of Piepjohn et al. (2019).

904   Considering the presence of crustal-scale, NNE-dipping, hundreds (to thousands?) of
905 kilometers long (Timanian) thrust systems extending from the Barents Sea (and possibly from
906 onshore Russia) to central–eastern and southern Spitsbergen and the northwestern Norwegian
907 Barents Sea (Figure 5a–c) prior to the onset of E–W-oriented Caledonian contraction, it is probable
908 that such large structures would have (at least partially) been reactivated and/or overprinted during
909 subsequent tectonic events if suitably oriented. Under E–W contraction, WNW–ESE-striking,
910 dominantly NNE-dipping Timanian faults would be oriented at c. 30° to the direction of principal
911 stress and, therefore, be suitable (according to Anderson's stress model) to reactivate/be
912 overprinted with sinistral strike-slip movements. Such kinematics were recorded along the
913 Vimsodden–Kosibapasset Shear Zone in Wedel Jarlsberg Land (Mazur et al., 2009) and within
914 Hornsund (von Gosen and Piepjohn, 2001).

915   However, recent ^{40}Ar–^{39}Ar geochronological determinations on muscovite within this
916 structure suggest that this structure formed during the Caledonian Orogeny (Faehnrich et al. 2020).
917 Nonetheless, the same authors also obtained Timanian ages (600–540 Ma) for (initial) movements
918 along minor shear zones nearby and parallel to the Vimsodden–Kosibapasset Shear Zone. Since
919 this large shear zone must have represented a major preexisting zone of weakness when Caledonian
920 contraction initiated, it is highly probable that it was preferentially chosen to reactivate instead of
921 minor shear zones. Thus, the Caledonian ages obtained along the Vimsodden–Kosibapasset Shear
922 Zone most likely reflect complete resetting of the geochronometer along the shear zone due to large
923 amounts of Caledonian reactivation–overprinting, while minor nearby shear zones preserved traces
924 of initial Timanian deformation. This is also supported by observations in northern Norway
925 suggesting that Timanian thrusts (e.g., Trollfjorden–Komagelva Fault Zone) were reactivated as

926   major strike-slip faults during the Caledonian Orogeny (Roberts, 1972; Herrevold et al., 2009; Rice
927   2014). This interpretation reconciles the strong differences in dipping angle and depth between the
928   Kinnhøgda–Daudbjørnpynten fault zone and the Vimsodden–Kosibapasset Shear Zone. The
929   former was located away from the Caledonian collision zone and essentially retained its initial,
930   moderately NNE-dipping Timanian geometry and was deeply buried during the Phanerozoic,
931   whereas the latter was intensely deformed, pushed into a sub-vertical position, and uplifted an
932   exhumed to the surface because it was located near or within the Caledonian collision zone.

933   This further explains why Timanian faults were not reactivated exclusively as strike-slip
934   faults despite being oriented sub-orthogonal (c. 70°) to E–W Caledonian contraction. Portions of
935   Timanian faults near the Caledonian collision zone were locally deformed into subvertical
936   geometries suitable to accommodate lateral movement, whereas their counterparts retaining their
937   moderate–low-angle dip away from the paleo-plate boundary were more prone to accommodate
938   vertical movements. Moreover, lateral transport of rocks from the Caledonian collision front
939   towards the inner portions of the Barents Sea in the east was hampered by rock units constituting
940   the crust of the Barents Sea, northern Norway, northwestern Russia and other adjacent areas.
941   Hence, Caledonian E–W contraction produced more easily N–S-trending folds (e.g., Figure 3b and
942   e and Figure 4f), which extended almost all the way to Novaya Zemlya (Figure 5), whereas partial
943   strike-slip reactivation was restricted to areas proximal to the Caledonian collision front (e.g.,
944   western Spitsbergen; Majka et al., 2008; Mazur et al., 2009; Faehnrich et al., 2020; Ziemniak et
945   al., 2020).

946

947   *Devonian–Carboniferous normal overprint–reactivation*

948   In Nordmannsfonna, the wedge shape of Devonian (–Mississippian?) sedimentary strata in
949   the hanging wall of the Kongsfjorden–Cowanodden fault zone suggest that the eastern portion of
950   this thrust was reactivated as a gently–moderately dipping extensional detachment (Figure 6c) and,
951   thus, that Devonian (–Mississippian?) strata in this area represent analogs to collapse deposits in
952   northern Spitsbergen. The intrusion of west-dipping Devonian (–Mississippian?) dykes orthogonal
953   to the eastern portion of the thrust system, i.e., orthogonal to extensional movements along the
954   inverted east-dipping portion of the thrust (Figure 3e and Figure 6d) also supports this
955   interpretation. Similar relationships were inferred in northwestern Spitsbergen, where Devonian

956 collapse sediments were deposited along a N–S-trending Precambrian basement ridge bounded by

957 a gently dipping, extensional mylonitic detachment (Braathen et al., 2018).

958 In Sassenfjorden, Storfjorden and the northeastern Norwegian Barents Sea, listric brittle

959 normal faults showing down-NNE offsets and syn-tectonic thickening within Devonian–

960 Carboniferous (–Permian?) sedimentary strata merge at depth with the uppermost part of NNE-

961 dipping Timanian thrust systems like the Kongsfjorden–Cowanodden fault zone (Figure 3a and d

962 and supplement S2c). This indicates that Timanian thrust systems were used as preexisting zones

963 of weakness during late–post-orogenic collapse of the Caledonides in the Devonian–Carboniferous

964 (Figure 6c–e and Figure 7c).

965 The presence of the Kongsfjorden–Cowanodden fault zone in Storfjorden and below

966 Edgeøya also explains the strong differences between the Paleozoic sedimentary successions

967 penetrated by the Plurdalen-1 and Raddendalen-1 exploration wells (Bro and Shvarts, 1983;

968 Harland and Kelly, 1997). Notably, the Plurdalen-1 well penetrated (at least) ca. 1600 meters thick

969 Devonian–Mississippian sedimentary rocks in the direct hanging wall of the Kongsfjorden–

970 Cowanodden fault zone and related listric brittle overprints (Figure 3a), whereas the interpretation

971 of Bro and Shvarts (1983) suggests that the Raddedalen-1 well encountered thin (90–290 meters

972 thick) Mississippian strata overlying (> 2 kilometers) thick lower Paleozoic sedimentary rocks ca.

973 30 kilometers farther northeast, i.e., away from the Kongsfjorden–Cowanodden fault zone and

974 related overprints. The presence of thick Devonian sedimentary strata in the direct hanging wall of

975 listric overprints of the Kongsfjorden–Cowanodden fault zone further supports late–post-

976 Caledonian extensional reactivation–overprinting of NNE-dipping Timanian thrusts.

977 In central Spitsbergen, recently identified Early Devonian–Mississippian normal faults

978 formed along and overprinted–reactivated major NNE-dipping ductile (mylonitic) shear zones and

979 fabrics in Billefjorden (Koehl et al., 2021 in review) and Sassenfjorden–Tempelfjorden (Koehl,

980 2020a). These show sizes, geometries and kinematics comparable to those of the Kongsfjorden–

981 Cowanodden fault zone, and are, therefore, interpreted as the western continuation of this thrust

982 system. The Devonian–Carboniferous extensional reactivation–overprinting of the Kongsfjorden–

983 Cowanodden fault zone in central Spitsbergen explains the southward provenance of northwards

984 prograding sedimentary rocks of the uppermost Silurian–Lower Devonian Siktefjellet and Red Bay

985 groups and Wood Bay Formation and the enigmatic WNW–ESE trend of the southern boundary of

986 the Devonian Graben in central–northern Spitsbergen (Gee and Moody-Stuart, 1966; Friend et al.,

987 1966; Friend and Moody-Stuart, 1972; Murascov and Mokin, 1979; Friend et al., 1997; McCann,

988 2000; Dallmann and Piepjohn, 2020; Koehl et al., 2021 in review).

989

990 *Mild Triassic overprint*

991   The Kongsfjorden–Cowanodden fault zone and associated overprints align with WNW–

992 ESE- to NW–SE-striking normal faults onshore southern and southwestern Edgeøya in

993 Kvalpynten, Negerpynten, and Øhmanfjellet (Osmundsen et al., 2014; Ogata et al., 2018). These

994 faults display both listric and steep planar geometries in cross-section and bound thickened syn-

995 sedimentary growth strata in lowermost Upper Triassic sedimentary rocks of the Tschermakfjellet

996 and De Geerdalen formations (Ogata et al., 2018; Smyrak-Sikora et al., 2020). The Norwegian

997 Barents Sea and Svalbard are believed to have remained tectonically quiet throughout the Triassic

998 apart from minor deep-rooted normal faulting in the northwestern Norwegian Barents Sea (Anell

999 et al., 2013) and Uralides-related contraction in the (south-) east (Müller et al., 2019). Hence, we

1000 propose that the progradation and accumulation of thick sedimentary deposits of the Triassic deltaic

1001 systems above the southeastward continuation of the Kongsfjorden–Cowanodden fault zone may

1002 have triggered minor tectonic adjustments resulting in the development of a system of small half-

1003 grabens over the thrust system. Alternatively or complementary, the deposition of thick Triassic

1004 deltaic systems may have locally accelerated compaction of sedimentary strata underlying the

1005 Tschermakjellet Formation in south- and southwest-Edgeøya, e.g., of the potential pre-Triassic

1006 syn-tectonic growth strata along the Kongsfjorden–Cowanodden fault zone, and, thus, facilitated

1007 the development of minor half-grabens within the Triassic succession along this thrust system.

1008

1009 *Eurekan reactivation–overprint*

1010   In eastern Spitsbergen, the Agardhbukta Fault segment of the Lomfjorden Fault Zone

1011 truncates the Kongsfjorden–Cowanodden fault zone with a major, > 0.5 second (TWT) top-west

1012 reverse offset (Figure 3e). The Agardhbukta fault also mildly folds Pennsylvanian–Mesozoic

1013 sedimentary rocks and Cretaceous sills into a gentle upright (fault-propagation) fold with no major

1014 offset (Figure 6f–g), which is supported by onshore field observations in eastern and northeastern

1015 Spitsbergen (Piepjohn et al., 2019). Mild folding of Mesozoic sedimentary rocks and of Cretaceous

1016 intrusions indicates that the Agardhbukta Fault was most likely mildly reactivated as a top-west

1017 thrust during the early Cenozoic Eurekan tectonic event (Figure 6g and Figure 7d).

1018   Seismic data show that high-angle listric Devonian–Carboniferous normal faults were
1019   mildly reactivated as reverse faults that propagated upwards and gently folded adjacent upper
1020   Paleozoic–Mesozoic (–Cenozoic?) sedimentary strata in the northwestern Norwegian Barents Sea,
1021   Storfjorden and central–eastern Spitsbergen (Figure 3a–c and supplement S2), but not in the
1022   northeastern Norwegian Barents Sea (Figure 3d). Since normal faults were not inverted in the east,
1023   it is probable that inversion of these faults in central–eastern Spitsbergen, Storfjorden and the
1024   northwestern Norwegian Barents Sea first occurred during the Eurekan tectonic event in the early
1025   Cenozoic, when Greenland collided with western Spitsbergen (Figure 7d). This is also supported
1026   by the gently folded character of Devonian–Mesozoic (–Cenozoic?) sedimentary successions in
1027   the west (Figure 3a and c), whereas these successions are essentially flat-lying (i.e., undeformed)
1028   in the east (Figure 3b and d). Nevertheless, folding of the seafloor reflection in Storfjorden and the
1029   northwestern Norwegian Barents Sea suggests ongoing contractional deformation along several of
1030   these faults in the northwestern Norwegian Barents Sea and Storfjorden (Figure 3a–c).

1031   Major, top-SSW mylonitic shear zones in Sassenfjorden–Tempelfjorden and Billefjorden
1032   display early Cenozoic overprints including top-SSW duplexes in uppermost Devonian–
1033   Mississippian coals of the Billefjorden Group acting as a partial décollement along a major
1034   basement-seated listric brittle fault (Koehl, 2020a; supplement S2) and NNE-dipping brittle faults
1035   offsetting the east-dipping Billefjorden Fault Zone by hundreds of meters to several kilometers left-
1036   laterally (Koehl et al., 2021 in review). Thus, the correlation of the Kongsfjorden–Cowanodden
1037   fault zone with these top-SSW mylonitic shear zones in Sassenfjorden–Tempelfjorden and
1038   Billefjorden (see Figure 1c for location) supports reactivation–overprinting of major NNE-dipping
1039   Timanian thrust systems as top-SSW, sinistral-reverse, oblique-slip thrusts in the early Cenozoic
1040   Eurekan tectonic event. Such correlation explains the NW–SE trend and the location of the
1041   northeastern boundary of the Central Tertiary Basin, which terminates just southwest of
1042   Sassenfjorden and Sassendalen in central Spitsbergen (Figure 1b–c). It also explains the dominance
1043   of NW–SE- to WNW–ESE-striking faults within Cenozoic deposits of the Central Tertiary Basin
1044   (Livshits, 1965a), and the northwestwards provenance (Petersen et al., 2016) and northwards
1045   thinning of sediments deposited in the basin (Livshits, 1965b), which were probably sourced from
1046   uplifted areas in the hanging wall of the reactivated–overprinted thrust.

1047   Noteworthy, Livshits (1965a) argued that the Central Tertiary Basin was bounded to the
1048   north by a major WNW–ESE-striking fault extending from Kongsfjorden to southern Billefjorden–

1049 Sassenjorden where the NNE-dipping Kongsfjorden–Cowanodden fault zone was mapped (present

1050 study; supplement S2). This indicates that the Kongsfjorden–Cowanodden fault zone might extend

1051 west of Billefjorden and Sassenfjorden, potentially until Kongsfjorden (see Figure 1c for location).

1052 Should it be the case, the Kongsfjorden–Cowanodden fault zone would coincide with a major

1053 terrane boundary in Svalbard, which was speculated to correspond to one or more regional WNW–

1054 ESE- to N–S-striking faults in earlier works, e.g., Kongsvegen Fault and Lapsdalen Thrust

1055 (Harland and Horsfield, 1974), Kongsvegen Fault Zone and/or Central–West Fault Zone (Harland

1056 and Wright, 1979), and Kongsfjorden–Hansbreen Fault Zone (Harland et al., 1993). The presence

1057 of a major, (inherited Timanian) NNE-dipping, basement-seated fault zone in this area would

1058 explain the observed strong differences between Precambrian basement rocks in Svalbard's

1059 northwestern and southwestern terranes.

1060 In southern Spitsbergen, von Gosen and Piepjohn (2001) and Bergh and Grogan (2003)

1061 suggested the presence of a WNW–ESE-striking, sinistral-reverse strike-slip fault in Hornsund

1062 based on a one-kilometer left-lateral offset of Devonian–Carboniferous sedimentary successions

1063 and of the early Cenozoic Hyrnefjellet Anticline across the fjord. This fault is part of the

1064 Kinnhøgda–Daudbjørnpynten fault zone and was most likely reactivated–overprinted during

1065 Eurekan contraction–transpression in the early Cenozoic.

1066

1067 *Present day tectonism*

1068 Seismic data show that the seafloor reflection is folded and/or offset in a reverse fashion by

1069 high-angle brittle faults merging at depth with interpreted Timanian thrust systems in Storfjorden

1070 and just north of Bjørnøya in the northwestern Norwegian Barents (Figure 3a and c, and Figure

1071 4h). This indicates that some of the Timanian thrust systems are still active at present and are

1072 reactivated/overprinted by reverse faults (Figure 7e). A potential explanation for ongoing

1073 reactivation–overprinting is transfer of extensional tectonic stress in the Fram Strait as ridge-push

1074 tectonism through Spitsbergen and Storfjorden.

1075

1076 **Implication for plate tectonics reconstructions of the Barents Sea and Svalbard in the late**

1077 **Neoproterozoic–Paleozoic**

1078 The presence of hundreds to thousands of kilometers long Timanian faults throughout the

1079 northern Norwegian Barents Sea and central and southwestern (and possibly northwestern?)

Spitsbergen indicates that the northwestern, northeastern and southwestern basement terranes of the Svalbard Archipelago were most likely already accreted together and attached to the Barents Sea, northern Norway and northwestern Russia in the late Neoproterozoic (ca. 600 Ma). Svalbard's three terranes were previously thought to have been juxtaposed during the Caledonian and Ellesmerian orogenies through hundreds–thousands of kilometers of displacement along presumed thousands of kilometers long N–S-striking strike-slip faults like the Billefjorden Fault Zone (Harland, 1969; Harland et al. 1992, Labrousse et al., 2008; Figure 2). The presence of laterally continuous (undisrupted), hundreds–thousands of kilometers long, Timanian thrust systems from southwestern and central Spitsbergen to the northern Norwegian and Russian Barents Sea clearly shows that this is not possible (Figure 8).

The continuous character of these thrust systems from potentially as far as onshore northwestern Russia through the Barents Sea and Svalbard precludes any major strike-slip displacement along N–S-striking faults such as the Billefjorden Fault Zone and Lomfjorden Fault Zone (as proposed by Harland et al., 1974, 1992; Labrousse et al., 2008; Figure 2) and any hard-linked connection between these faults in Svalbard and analogous, NE–SW-striking faults in Scotland in the Phanerozoic (as proposed by Harland, 1969). Instead, the present work suggests that the crust constituting the Barents Sea and the northeastern and southwestern basement terranes of Svalbard should be included as part of Baltica in future Arctic plate tectonics reconstructions for the late Neoproterozoic–Paleozoic period (i.e., until ca. 600 Ma; Figure 8). It also suggests that the Caledonian suture zone, previously inferred to lie east of Svalbard in the Barents Sea (e.g., Gee and Teben'kov, 2004; Breivik et al., 2005; Barrère et al., 2011; Knudsen et al., 2019) may be located west of the presently described Timanian thrust systems, i.e., probably west of or in western Spitsbergen where Caledonian blueschist and eclogite metamorphism has been recorded in Precambrian basement rocks (Horsfield, 1972; Dallmeyer et al., 1990a; Ohta et al., 1995; Kosminska et al., 2014).

Conclusions

1) Seismic data in the northern Norwegian Barents Sea and Svalbard reveal the existence of several systems of hundreds–thousands of kilometers long, several kilometers thick, top-SSW thrusts comprised of brittle–ductile thrusts, mylonitic shear zones and associated SSW-verging folds that appear to extend from onshore northwestern Russia to the northern

Norwegian Barents Sea and to central and southwestern Spitsbergen. A notable structure is the Kongsfjorden–Cowanodden fault zone in Svalbard and the Norwegian Barents Sea, which likely merges with the Baidaratsky fault zone in the Russian Barents Sea and southern Novaya Zemlya. We interpret these thrust systems as being related to the Neoproterozoic Timanian Orogeny.

2) In the east (away from the Caledonian collision zone), these Timanian thrusts systems were folded into NNE-plunging folds, offset, and reactivated as and/or overprinted by top-west, oblique-slip sinistral-reverse, brittle–ductile thrusts during subsequent Caledonian (e.g., Agardhbukta Fault segment of the Lomfjorden Fault Zone) and, possibly, during Eurekan contraction, and are deeply buried. By contrast, in the west (near or within the Caledonian collision zone), Timanian thrusts were intensely deformed, pushed into sub-vertical positions, extensively overprinted, and exhumed to the surface.

3) In eastern Spitsbergen, a major NNE-dipping Timanian thrust system, the Kongsfjorden–Cowanodden fault zone, is crosscut by a swarm of Devonian (–Mississippian?) dykes that intruded contemporaneous sedimentary strata deposited during extensional reactivation of the eastern portion of the thrust system as a low-angle extensional detachment during late–post-Caledonian collapse.

4) Timanian thrust systems were overprinted by NNE-dipping, brittle normal faults in the late Paleozoic during the collapse of the Caledonides and/or subsequent rifting in the Devonian–Carboniferous.

5) Timanian thrust systems and associated Caledonian and Devonian–Carboniferous brittle overprints (e.g., Agardhbukta Fault) in the northwestern Norwegian Barents Sea and Svalbard were mildly reactivated during the early Cenozoic Eurekan tectonic event, which resulted in minor folding and minor reverse offsets of Devonian–Mesozoic sedimentary strata and intrusions. Timanian thrusts and related overprints in the northeastern Norwegian Barents Sea were not reactivated during the Eurekan tectonic event.

6) The presence of hundreds–thousands of kilometers long Timanian thrust systems may suggest that the Barents Sea and Svalbard's three basement terranes were already attached to northern Norway and northwestern Russia in the late Neoproterozoic (ca. 600 Ma). If correct, a Timanian origin for these structures would preclude any major strike-slip movements along major N–S-striking faults like the Billefjorden and Lomfjorden fault

1142 zones in the Phanerozoic, and imply that the Caledonian suture zone is located west of or
1143 in western Spitsbergen.

1144

1145 **Acknowledgements**

1146 The present study was supported by the Research Council of Norway, the Tromsø Research
1147 Foundation, and six industry partners through the Research Centre for Arctic Petroleum
1148 Exploration (ARCEx; grant number 228107), the SEAMSTRESS project (grant number 287865),
1149 and the Centre for Earth Evolution and Dynamics (CEED; grant number 223272). We thank the
1150 Norwegian Petroleum Directorate and the Federal Institute for Geosciences and Natural Resources
1151 (BGR) for granting access and allowing publication of seismic, magnetic and gravimetric data in
1152 Svalbard and the Norwegian Barents Sea. Prof. Steffen Bergh, Dr. Winfried Dallmann, Prof. Jiri
1153 Konopasek, Assoc. Prof. Mélanie Forien, Dr. Kate Waghorn (UiT The Arctic University of Norway
1154 in Tromsø), Dr. Peter Klitzke (Federal Institute for Geosciences and Natural Resources –
1155 Germany), Anna Dichiarante (Norway Seismic Array), Rune Mattingsdal (Norwegian Petroleum
1156 Directorate), and Prof. Carmen Gaina (Centre for Earth Evolution and Dynamics, University of
1157 Oslo) are thanked for fruitful discussion.

1158

1159 **Data availability**

1160 For high-resolution versions of the figures and supplements, the reader is referred to the
1161 Open Access data repository DataverseNO (doi.org/10.18710/CE8RQH).

1162

1163 **References**

1164 Aakvik, R.: Fasies analyse av Undre Karbonske kullførende sedimenter, Billefjorden, Spitsbergen,
1165   Ph.D. Thesis, University of Bergen, Bergen, Norway, 219 pp., 1981.
1166 Andresen, A., Haremo, P., Swensson, E. and Bergh, S. G.: Structural geology around the southern
1167   termination of the Lomfjorden Fault Complex, Agardhdalen, east Spitsbergen, Norsk Geol.
1168   Tidsskr., 72, 83–91, 1992.
1169 Anell, I., Braathen, A., Olaussen, S. and Osmundsen, P. T.: Evidence of faulting contradicts a
1170   quiescent northern Barents Shelf during the Triassic, First Break, 31, 67–76, 2013.
1171 Anell, I. M., Braathen, A. and Olaussen, S.: Regional constraints of the Sørkapp Basin: A
1172   Carboniferous relic or a Cretaceous depression, Mar. Petrol. Geol., 54, 123–138, 2014.

1173 Anell, I. M., Faleide, J. I. and Braathen, A.: Regional tectono-sedimentary development of the
1174   highs and basins of the northwestern Barents Shelf, Norsk Geologisk Tidsskrift, 96, 1, 27–
1175   41, 2016.

1176 Arbaret, L. and Burg, J.-P.: Complex flow in lowest crustal, anastomosing mylonites: Strain
1177   gradients in a Kohistan gabbro, northern Pakistan, J. Geophys. Res., 108, 2467, 2003.

1178 Barrère, C., Ebbing, J. and Gernigon, L.: Offshore prolongation of Caledonian structures and
1179   basement characterization in the western Barents Sea from geophysical modelling,
1180   Tectonophys., 470, 71–88, 2009.

1181 Barrère, C., Ebbing, J. and Gernigon, L.: 3-D density and magnetic crustal characterization of the
1182   southwestern Barents Shelf: implications for the offshore prolongation of the Norwegian
1183   Caledonides, Geophys. J. Int., 184, 1147–1166, 2011.

1184 Boyer, S. E. and Elliott, D.: Thrust Systems, AAPG Bulletin, 66, 9, 1196–1230, 1982.

1185 Braathen, A., Bælum, K., Maher Jr., H. D. and Buckley, S. J.: Growth of extensional faults and
1186   folds during deposition of an evaporite-dominated half-graben basin; the Carboniferous
1187   Billefjorden Trough, Svalbard, Norsk Geol. Tidsskr., 91, 137–160, 2011.

1188 Braathen, A., Osmundsen, P. T., Maher, H. and Ganerød, M.: The Keisarhjelmen detachment
1189   records Silurian–Devonian extensional collapse in Northern Svalbard, Terra Nova, 30, 34–
1190   39, 2018.

1191 Breivik, A. J., Mjelde, R., Grogan, P., Shimamura, H., Murai, Y. and Nishimura, Y.: Caledonide
1192   development offshore–onshore Svalbard based on ocean bottom seismometer, conventional
1193   seismic, and potential field data, Tectonophys., 401, 79–117, 2005.

1194 Bro, E. G. and Shvarts, V. H.: Processing results from drill hole Raddedalen-1, Edge Island,
1195   Spitzbergen Archipelago, All-Russian Research Institute for Geology and Mineral
1196   Resources of the World Ocean, St. Petersburg, Pangaea, Report 5750, 1983.

1197 Cawood, P. A., McCausland, P. J. A. and Dunning, G. R.: Opening Iapetus: Constraints from the
1198   Laurentian margin in Newfoundland, GSA Bull., 113, 4, 443–453, 2001.

1199 Chalmers, J. A. and Pulvertaft, T. C. R.: Development of the continental margins of the Labrador
1200   Sea: a review, in: Non-Volcanic Rifting of Continental Margins: A Comparison of
1201   Evidence from Land and Sea, edited by: Wilson, R. C. L., Taylor, R. B. and Froitzheim,
1202   N., Geol. Soc. London, Spec. Publi., 187, 77–105, 2001.

Cocks, L. R. M. and Torsvik, T. H.: Baltica from the late Precambrian to mid-Palaeozoic times: The gain and loss of a terrane's identity, Earth-Sci. Rev., 72, 39–66, 2005.

Colombu, S., Cruciani, G., Fancello, D., Franceschelli, M. and Musumeci, G.: Petrophysical properties of a granite-protomylonite-ultramylonite sequence: insight from the Monte Grighini shear zone, central Sardinia, Italy, Eur. J. Mineral, 27, 471–486, 2015.

Corfu, F., Andersen, T. B. and Gasser, D.: The Scandinavian Caledonides: main features, conceptual advances and critical questions, in: New Perspectives on the Caledonides of Scandinavia and Related Areas, edited by: Corfu, F., Gasser, D. and Chew, D. M., Geol. Soc., London, Spec. Publi., 390, 9–43, 2014.

Cutbill, J. L. and Challinor, A.: Revision of the Stratigraphical Scheme for the Carboniferous and Permian of Spitsbergen and Bjørnøya, Geol. Mag., 102, 418–439, 1965.

Cutbill, J. L., Henderson, W. G. and Wright, N. J. R.: The Billefjorden Group (Early Carboniferous) of central Spitsbergen, Norsk Polarinst. Skr., 164, 57–89, 1976.

Dallmann, W. K.: Geoscience Atlas of Svalbard, Norsk Polarinstitutt, Tromsø, Norway, Rapportserie nr. 148, 2015.

Dallmann, W. K. and Krasil'scikov, A. A.: Geological map of Svalbard 1:50,000, sheet D20G Bjørnøya, Norsk Polarinst. Temakart, 27, 1996.

Dallmann, W. K. and Piepjohn, K.: The structure of the Old Red Sandstone and the Svalbardian Orogenic Event (Ellesmerian Orogeny) in Svalbard, Norg. Geol. Unders. B., Spec. Publi., 15, 106 pp., 2020.

Dallmeyer, R. D., Peucat, J. J., Hirajima, T. and Ohta, Y.: Tectonothermal chronology within a blueschist–eclogite complex, west-central Spitsbergen, Svalbard: Evidence from ^{40}Ar/^{39}Ar and Rb–Sr mineral ages, Lithos, 24, 291–304, 1990a.

Dallmeyer, R. D., Peucat, J. J. and Ohta, Y.: Tectonothermal evolution of contrasting metamorphic complexes in northwest Spitsbergen (Biskayerhalvøya): Evidence from ^{40}Ar/^{39}Ar and Rb-Sr mineral ages, GSA Bull., 102, 653–663, 1990b.

Dewey, J. F. and Strachan, R. A.: Changing Silurian–Devonian relative plate motion in the Caledonides: sinistral transpression to sinistral transtension, J. Geol. Soc., London, 160, 219–229, 2003.

Drachev, S. S.: Fold belts and sedimentary basins of the Eurasian Arctic, Arktos, 2:21, 2016.

Drachev, S. S., Malyshev, N. A. and Nikishin, A. M.: Tectonic history and petroleum geology of the Russian Arctic Shelves: an overview, Petrol. Geol. Conf. series, 7, 591–619, 2010.

Dumais, M.-A. and Brönner, M.: Revisiting Austfonna, Svalbard, with potential field methods – a new characterization of the bed topography and its physical properties, The Cryosphere, 14, 183–197, 2020.

Eldholm, O. and Ewing, J.: Marine Geophysical Survey in the Southwestern Barents Sea, J. Geophys. Res., 76, 17, 3832–3841, 1971.

Engen, Ø., Faleide, J. I. and Dyreng, T. K.: Opening of the Fram Strait gateway: A review of plate tectonic constraints, Tectonophys., 450, 51–69, 2008.

Estrada, S., Tessensohn, F. and Sonntag, B.-L.: A Timanian island-arc fragment in North Greenland: The Midtkap igneous suite, J. Geodyn., 118, 140–153, 2018.

Faehnrich, K., Majka, J., Schneider, D., Mazur, S., Manecki, M., Ziemniak, G., Wala, V. T. and Strauss, J. V.: Geochronological constraints on Caledonian strike-slip displacement in Svalbard, with implications for the evolution of the Arctic, Terra Nova, 2020, 32, 290–299.

Fortey, R. A. and Bruton, D. L.: Lower Ordovician trilobites of the Kirtonryggen Formation, Spitsbergen, ossils and Strata, 59, Wiley Blackwell, 120 pp., 2013.

Fountain, D. M., Hurich, C. A. and Smithson, S. B.: Seismic relectivity of mylonite zones in the crust, Geology, 12, 195–198, 1984.

Friend, P. F. and Moody-Stuart, M.: Sedimentation of the Wood Bay Formation (Devonian) of Spitsbergen: Regional analysis of a late orogenic basin, Norsk Polarinst. Skr., 157, 80 pp., 1972.

Friend, P. F., Heintz, N. and Moody-Stuart, M.: New unit terms for the Devonian of Spitsbergen and a new stratigraphical scheme for the Wood Bay Formation, Polarinst. Årbok, 1965, 59–64, 1966.

Friend, P. F., Harland, W. B., Rogers, D. A., Snape, I. and Thornley, R. S.: Late Silurian and Early Devonian stratigraphy and probable strike-slip tectonics in northwestern Spitsbergen, Geol. Mag., 134, 4, 459–479, 1997.

Gasser, D.: The Caledonides of Greenland, Svalbard and other Arctic areas: status of research and open questions, in: New Perspectives on the Caledonides of Scandinavia and Related Areas, edited by: Corfu, F., Gasser, D. and Chew, D. M., Geol. Soc., London, Spec. Publi., 390, 93–129, 2014.

Gee, D. G. and Moody-Stuart, M.: The base of the Old Red Sandstone in central north Haakon VII
Land, Vestspitsbergen, Polarinst. Årbok, 1964, 57–68, 1966.

Gee, D. G. and Pease, V.: The Neoproterozoic Timanide Orogen of eastern Baltica: introduction,
in: The Neoproterozoic Timanide Orogen of eastern Baltica, edited by: Gee, D. G. and
Pease, V., Geol. Soc. London, Mem., 30, 1–3, 2004.

Gee, D. G. and Teben'kov, A. M.: Svalbard: a fragment of the Laurentian margin, in: The
Neoproterozoic Timanide Orogen of eastern Baltica, edited by: Gee, D. G. and Pease, V.,
Geol. Soc. London, Mem., 30, 191–206, 2004.

Gee, D. G., Björklund, L and Stølen, L.-K.: Early Proterozoic basement in Ny Friesland–
implications for the Caledonian tectonics of Svalbard, Tectonophys., 231, 171–182, 1994.

Gee, D. G., Fossen, H., Henriksen, N. and Higgins, A. K.: From the Early Paleozoic Platforms of
Baltica and Laurentia to the Caledonide Orogen of Scandinavia and Greenland, Episodes,
31, 1, 44–51, 2008.

Gernigon, L. and Brönner, M.: Late Palaeozoic architecture and evolution of the southwestern
Barents Sea: insights from a new generation of aeromagnetic data, J. Geol. Soc., London,
169, 449–459, 2012.

Gernigon, L., Brönner, M., Roberts, D., Olesen, O., Nasuti, A. and Yamasaki, T.: Crustal and basin
evolution of the southwestern Barents Sea: From Caledonian orogeny to continental
breakup, Tectonics, 33, 347-373, 2014.

Gernigon, L., Brönner, M., Dumais, M.-A., Gradmann, S., Grønlie, A., Nasuti, A. and Roberts, D.:
Basement inheritance and salt structures in the SE Barents Sea: Insights from new potential
field data, J. Geodyn., 119, 82–106, 2018.

Griffin, W. L., Nikolic, N., O'Reilly, S. Y. and Pearson, N. J.: Coupling, decoupling and
metasomatism: Evolution of crust–mantle relationships beneath NW Spitsbergen, Lithos,
149, 115–135, 2012.

Gudlaugsson, S. T., Faleide, J. I., Johansen, S. E. and Breivik, A. J.: Late Palaeozoic structural
development of the South-western Barents Sea. Mar. Petrol. Geol., 15, 73–102, 1998.

Haremo, P. and Andresen, A.: Tertiary décollements thrusting and inversion structures along
Billefjorden and Lomfjorden Fault Zones, East Central Spitsbergen, in: Structural and
Tectonic Modelling and its Apllication to Petroleum Geology, edited by: Larsen, R. M.,

Brekke, H., Larsen, B. T. and Talleraas, E., Norwegian Petroleum Society (NPF) Special Publications, 1, 481–494, 1992.

Harland, W. B.: Contribution of Spitsbergen to understanding of tectonic evolution of North Atlantic region, AAPG Memoirs, 12, 817–851, 1969.

Harland, W. B. and Horsfield, W. T.: West Spitsbergen Orogen, in: Mesozoic–Cenozoic Orogenic Belts, data for Orogenic Studies, J. Geol. Soc. London, Spec. Publi., 4, 747–755, 1974.

Harland, W. B. and Kelly, S. R. A.: Eastern Svalbard Platform, in: Geology of Svalbard, edited by: Harland, W. B., Geol. Soc. London, Mem., 17, 521 pp., 1997.

Harland, W. B. and Wright, N. J. R.: Alternative hypothesis for the pre-Carboniferous evolution of Svalbard, Norsk Polarinst. Skr., 167, 89–117, 1979.

Harland, W. B., Cutbill, L. J., Friend, P. F., Gobbett, D. J., Holliday, D. W., Maton, P. I., Parker, J. R. and Wallis, R. H.: The Billefjorden Fault Zone, Spitsbergen – the long history of a major tectonic lineament, Norsk Polarinst. Skr., 161, 1–72, 1974.

Harland, W. B., Scott, R. A., Auckland, K. A. and Snape, I.: The Ny Friesland Orogen, Spitsbergen, Geol. Mag., 129, 6, 679–708, 1992.

Harland, W. B., Hambrey, M. J. and Waddams, P.: Vendian geology of Svalbard, Norsk Polarinst. Skri., 193, 152 pp., 1993.

Hassaan, M.: Evaporite-influenced rift basins and salt tectonics in the southeastern Norwegian Barents Sea, Ph.D. Thesis, University of Oslo, Oslo, Norway, 305 pp., 2021.

Hassaan, M., Faleide, J. I., Gabrielsen, R. H. and Tsikalas, F.: Carboniferous graben structures, evaporite accumulations and tectonic inversion in the southeastern Norwegian Barents Sea, Mar. Petrol. Geol., 112, 104038, 2020a.

Hassaan, M., Faleide, J. I., Gabrielsen, R. H. and Tsikalas, F.: Architecture of the evaporite accumulation and salt structures dynamics in Tiddlybanken Basin, southeastern Norwegian Barents Sea, Basin Res., 33, 91–117, 2020b.

Hassaan, M., Faleide, J. I., Gabrielsen, R. H. and Tsikalas, F.: Effects of basement structures and Carboniferous basin configuration on evaporite distribution and the development of salt structures in Nordkapp Basin, Barents Sea—Part I, Basin Res., 33, 4, 2474–2499, 2021.

Herrevold, T., Gabrielsen, R. H. and Roberts, D.: Structural geology of the southeastern part of the Trollfjorden-Komagelva Fault Zone, Varanger Peninsula, Finnmark, North Norway, Norwegian Journal of Geology, 89, 305-325, 2009.

Horsfield, W. T.: Glaucophane schists of Caledonian age from Spitsbergen, Geol. Mag., 109, 1, 29–36, 1972.

Hurich, C. A., Smithson, S. B., Fountain, D. M. and Humphreys, M. C.: Seismic evidence of mylonite reflectivity and deep structure in the Kettle dome metamorphic core complex, Washington, Geology, 13, 577–580, 1985.

Jakobsson, M., Mayer, L., Coackley, B., Dowdeswell, J. A., Forbes, S., Fridman, B., Hodnesdal, H., Noormets, R., Pedersen, R., Rebesco, M., Schenke, H. W., Zarayskaya, Y., Accettella, D., Armstrong, A., Anderson, R. M., Bienhoff, P., Camerlenghi, A., Church, I., Edwards, M., Gardner, J. V., Hall, J. K., Hell, B., Hestvik, O., Kristoffersen, Y., Marcussen, C., Mohammad, R., Mosher, D., Nghiem, S. V., Pedrosa, M. T., Travaglini, P. G., and Weatherall, P.: The International Bathymetric Chart of the Arctic Ocean (IBCAO) Version 3.0, Geophys. Res. Lett., 39, L12609, https://doi.org/10.1029/2012GL052219, 2012.

Johansen, S. E., Ostisty, B. K., Birkeland, Ø., Fedorovsky, Y. F., Martirosjan, V. N., Bruun Christensen, O., Cheredeev, S. I., Ignatenko, E. A. and Margulis, L. S.: Hydrocarbon potential in the Barents Sea region: play distribution and potential, in: Arctic Geology and Petroleum Potential, edited by: Vorren, T. O., Bergsager, E., Dahl-Stamnes, Ø. A., Holter, E., Johansen, B., Lie, E. and Lund, T. B., NPF Spec. Publi., 2, 273–320, Elsevier, Amsterdam, 1992.

Johansson, Å., Larionov, A. N., Gee, D. G., Ohta, Y., Tebenkov, A. M. and Sandelin, S.: Greenvillian and Caledonian tectono-magmatic activity in northeasternmost Svalbard, in: The Neoproterozoic Timanide Orogen of Eastern Baltica, edited by: Gee, D. G. and Pease, V., Geol. Soc. London Memoirs, 30, 207–232, 2004.

Johansson, Å., Gee, D. G., Larionov, A. N., Ohta, Y. and Tebenkov, A. M.: Greenvillian and Caledonian evolution of eastern Svalbard – a tale of two orogenies, Terra Nova, 17, 317–325, 2005.

Kairanov, B., Escalona, A., Mordascova, A., Sliwinska, K. and Suslova, A.: Early Cretaceous tectonostratigraphy evolution of the north central Barents Sea, J. Geodyn., 119, 183–198, 2018.

Klitzke, P., Franke, D., Ehrhardt, A., Lutz, R., Reinhardt, L., Heyde, I. and Faleide, J. I.: The Palaeozoic Evolution of the Olga Basin Region, Northern Barents Sea: A Link to the Timanian Orogeny, Geochem., Geophy., Geosy., 20, 614–629, 2019.

Knudsen, C., Gee, D. G., Sherlock, S. C. and Yu, L.: Caledonian metamorphism of metasediments from Franz Josef Land, GFF, 141, 295–307, 2019.

Koehl, J.-B. P.: Early Cenozoic Eurekan strain partitioning and decoupling in central Spitsbergen, Svalbard, Solid Earth, 12, 1025–1049, 2020a.

Koehl, J.-B. P.: Impact of Timanian thrusts on the Phanerozoic tectonic history of Svalbard, Keynote lecture, EGU General Assembly, May 3rd–8th 2020, Vienna, Austria, 2020b.

Koehl, J.-B. P. and Muñoz–Barrera, J. M.: From widespread Mississippian to localized Pennsylvanian extension in central Spitsbergen, Svalbard, Solid Earth, 9, 1535–1558, 2018.

Koehl, J.-B. P., Bergh, S. G., Henningsen, T. and Faleide, J. I.: Middle to Late Devonian–Carboniferous collapse basins on the Finnmark Platform and in the southwesternmost Nordkapp basin, SW Barents Sea, Solid Earth, 9, 341–372, 2018.

Koehl, J.-B. P., Bergh, S. G., Osmundsen, P. T., Redfield, T., Indrevær, K., Lea. H. and Bergø, E.: Late Devonian–Carboniferous faulting and controlling structures and fabrics in NW Finnmark, Norw. J. Geol., 99, 3, 1–40, 2019.

Koehl, J.-B. P., Allaart, L. and Noormets, R.: Devonian–Carboniferous collapse and segmentation of the Billefjorden Trough, and Eurekan inversion–overprint and strain partitioning and decoupling along inherited WNW–ESE-striking faults, in review, 2021.

Korago, E. A., Kovaleva, G. N., Lopatin, B. G. and Orgo, V. V.: The Precambrian rocks of Novaya Zemlya, in: The Neoproterozoic Timanide Orogen of Eastern Baltica, edited by: Gee, D. G. and Pease, V., Geol. Soc. London, Mem., 30, 135–143, 2004.

Kosminska, K., Majka, J., Mazur, S., Krumbholz, M., Klonowska, I., Manecki, M., Czerny, J. and Dwornik, M.: Blueschist facies metamorphism in Nordenskiöld Land of west-central Svalbard, Terra Nova, 26, 377–386, 2014.

Kostyuchenko, A., Sapozhnikov, R., Egorkin, A., Gee, D. G., Berzin, R. and Solodilov, L.: Crustal structure and tectonic model of northeastern Baltica, based on deep seismic and potential field data, in: European Lithosphere Dynamics, edited by: Gee, D. G. and Stephenson, R. A., Geol. Soc. London Mem., 32, 521–539, 2006.

Labrousse, L., Elvevold, S., Lepvrier, C. and Agard, P.: Structural analysis of high-pressure metamorphic rocks of Svalbard: Reconstructing the early stages of the Caledonian orogeny, Tectonics, 27, 22 pp., 2008.

1386 Lamar, D. L. and Douglass, D. N.: Geology of an area astride the Billefjorden Fault Zone, Northern
1387   Dicksonland, Spitsbergen, Svalbard, Polarist. Skr., 197, 46 pp., 1995.

1388 Lamar, D. L., Reed, W. E. and Douglass, D. N.: Billefjorden fault zone, Spitsbergen: Is it part of a
1389   major Late Devonian transform?, GSA, 97, 1083–1088, 1986.

1390 Larssen, G. B., Elvebakk, G., Henriksen, L. B., Kristensen, S.-E., Nilsson, I., Samuelsberg, T. J.,
1391   Svånå, T. A., Stemmerik, L. and Worsley, D.: Upper Palaeozoic lithostratigraphy of the
1392   Southern part of the Norwegian Barents Sea, Norges geol. unders. Bull., 444, 45 pp., 2005.

1393 Lasabuda, A., Laberg, J. S., Knutsen, S.-M. and Safronova, P.: Cenozoic tectonostratigraphy and
1394   pre-glacial erosion: A mass-balance study of the northwestern Barents Sea margin,
1395   Norwegian Arctic, J. Geodyn., 119, 149–166, 2018.

1396 Lippard, S. J. and Prestvik, T.: Carboniferous dolerite dykes on Magerøy: new age determination
1397   and tectonic significance, Norsk Geologisk Tidsskrift, 77, 159-163, 1997.

1398 Livshits, Yu. Ya.: Tectonics of Central Vestspitsbergen, in: Geology of Spitsbergen, edited by:
1399   Sokolov, V. N., National Lending Library of Science and Technology, Boston Spa.,
1400   Yorkshire, UK, 59–75, 1965a.

1401 Livshits, Yu. Ya.: Paleogene deposits of Nordenskiöld Land, Vestspitsbergen, in: Geology of
1402   Spitsbergen, edited by: Sokolov, V. N., National Lending Library of Science and
1403   Technology, Boston Spa., Yorkshire, UK, 193–215, 1965b.

1404 Lopatin, B. G., Pavlov, L. G., Orgo, V. V. and Shkarubo, S. I.: Tectonic Structure of Novaya
1405   Zemlya, Polarforschung, 69, 131–135, 2001.

1406 Lorenz, H., Pystin, A. M., Olovyanishnikov, V. G. and Gee, D. G.: Neoproterozoic high-grade
1407   metamorphism of the Kanin Peninsula, Timanide Orogen, northern Russia, in: The
1408   Neoproterozoic Timanide Orogen of Eastern Baltica, edited by: Gee, D. G. and Pease, V.,
1409   Geol. Soc. London, Mem., 30, 59–68, 2004.

1410 Lorenz, H., Männik, P., Gee, D. and Proskurnin, V.: Geology of the Severnaya Zemlya Archipelao
1411   and the North Kara Terrane in the Russian high Arctic, Int. J. Earth Sci., 97, 519–547, 2008.

1412 Lowell, J. D.: Spitsbergen tertiary Orogenic Belt and the Spitsbergen Fracture Zone, GSA Bull.,
1413   83, 3091–3102, 1972.

1414 Lyberis, N. and Manby, G.: Continental collision and lateral escape deformation in the lower and
1415   upper crust: An example from Caledonide Svalbard, Tectonics, 18, 1, 40–63, 1999.

1416 Majka, J. and Kosminska, K.: Magmatic and metamorphic events recorded within the Southwestern
1417   Basement Province of Svalbard, Arktos, 3:5, 2017.

1418 Majka, J., Mazur, S., Manecki, M., Czerny, J. and Holm, D. K.: Late Neoproterozoic amphibolite-
1419   facies metamorphism of a pre-Caledonian basement block in southwest Wedel Jarlsberg
1420   Land, Spitsbergen: new evidence from U–Th–Pb dating of monazite, Geol. Mag., 145, 6,
1421   822–830, 2008.

1422 Majka, J., Larionov, A. N., Gee, D. G., Czerny, J. and Prsek, J.: Neoproterozoic pegmatite from
1423   Skoddefjellet, Wedel Jarlsberg Land, Spitsbergen: Additional evidence for c. 640 Ma
1424   tectonothermal event in the Caledonides of Svalbard, Polish Polar Res., 33, 1–17, 2012.

1425 Majka, J., De'eri-Shlevin, Y., Gee, D. G., Czerny, J., Frei, D. and Ladenberger, A.: Torellian (c.
1426   640 Ma) metamorphic overprint of Tonian (c. 950 Ma) basement in the Caledonides of
1427   southwestern Svalbard, Geol. Mag., 151, 4, 732–748, 2014.

1428 Manby, G. M. and Lyberis, N.: Tectonic evolution of the Devonian Basin of northern Spitsbergen,
1429   Norsk Geol. Tidsskr., 72, 7–19, 1992.

1430 Manby, G. M., Lyberis, N., Chorowicz, J. and Thiedig, F.: Post-Caledonian tectonics along the
1431   Billefjorden fault zone, Svalbard, and implications for the Arctic region, Geol. Soc. Am.
1432   Bul., 105, 201–216, 1994.

1433 Manecki, M., Holm, D. K., Czerny, J. and Lux, D.: Thermochronological evidence for late
1434   Proterozoic (Vendian) cooling in southwest Wedel Jarlsberg Land, Spitsbergen, Geological
1435   Magazine, 135, 63–9, 1998.

1436 Marello, L., Ebbing, J. and Gernigon, L.: Magnetic basement study in the Barents Sea from
1437   inversion and forward modelling, Tectonophys., 493, 153–171, 2010.

1438 Marello, L., Ebbing, J. and Gernigon, L.: Basement inhomogeneities and crustal setting in the
1439   Barents Sea from a combined 3D gravity and magnetic model, Geophys. J. Int., 193, 2,
1440   557–584, 2013.

1441 Mazur, S., Czerny, J., Majka, J., Manecki, M., Holm, D., Smyrak, A. and Wypych, A.: A strike-
1442   slip terrane boundary in Wedel Jarlsberg Land, Svalbard, and its bearing on correlations pf
1443   SW Spitsbergen with the Pearya terrane and Timanide belt, J. Geol. Soc. London, 166, 529–
1444   544, 2009.

1445 McCann, A. J.: Deformation of the Old Red Sandstone of NW Spitsbergen; links to the Ellesmerian
1446 and Caledonian orogenies, in: New Perspectives on the Old Red Sandstone, edited by:
1447 Friends, P. F. and Williams, B. P. J., Geol. Soc. London, 180, 567–584, 2000.

1448 Merdith, A. S., Williams, S. E., Collins, A. S., Tetley, M. G., Mulder, J. A., Blades, M. L., Young,
1449 A., Armistead, S. E., Cannon, J., Zahirovic, S. and Müller, R. D.: Extending full-plate
1450 tectonic models into deep time: Linking the Neoproterozoic and the Phanerozoic, Earth-
1451 Sci. Rev., 214, 103477, 2021.

1452 Müller, R., Klausen, T. G., Faleide, J. I., Olaussen, S., Eide, C. H. and Suslova, A.: Linking regional
1453 unconformities in the Barents Sea to compression-induced forebulge uplift at the Triassic-
1454 Jurassic transition, Tectonophys., 765, 35–51, 2019.

1455 Murascov, L. G. and Mokin, Ju. I.: Stratigraphic subdivision of the Devonian deposits of
1456 Spitsbergen, Polarinst. Skr., 167, 249–261, 1979.

1457 Nasuti, A., Roberts, D. and Gernigon, L.: Multiphase mafic dykes in the Caledonides of northern
1458 Finnmark revealed by a new high-resolution aeromagnetic dataset, Norwegian Journal of
1459 Geology, 95, 251-263, 2015.

1460 Norton, M. G., McClay, K. R. and Way, N. A.: Tectonic evolution of Devonian basins in northern
1461 Scotland and southern Norway, Norsk Geol. Tidsskr., 67, 323–338, 1987.

1462 Oakey, G. N. and Chalmers, J. A.: A new model for the Paleogene motion of Greenland relative to
1463 North America: Plate reconstructions of the Davis Strait and Nares Strait regions between
1464 Canada and Greenland, J. of Geophys. Res., 117, B10401, 2012.

1465 Ogata, K., Mulrooney, M. J., Braathen, A., Maher, H., Osmundsen, P. T., Anell, I., Smyrak-Sikora,
1466 A. A. and Balsamo, F.: Architecture, deformation style and petrophysical properties of
1467 growth fault systems: the Late Triassic deltaic succession of southern Edgeøya (East
1468 Svalbard), Basin Res., 30, 5, 1042–1073, 2018.

1469 Ohta, Y., Dallmeyer, R. D. and Peucat, J. J.: Caledonian terranes in Svalbard, GSA Spec. Paper,
1470 230, 1–15, 1989.

1471 Ohta, Y., Krasil'scikov, A. A., Lepvrier, C. and Teben'kov, A. M.: Northern continuation of
1472 Caledonian high-pressure metamorphic rocks in central-western Spitsbergen, Polar Res.,
1473 14, 3, 303–315, 1995.

1474 Olovyanishshnikov, V. G., Roberts, D. and Siedlecka, A.: Tectonics and Sedimentation of the
1475   Meso- to Neoproterozoic Timan-Varanger Belt along the Northeastern Margin of Baltica,
1476   Polarforschung, 68, 267–274, 2000.

1477 Osmundsen, P-T., Braathen, A., Rød, R. S. and Hynne, I. B.: Styles of normal faulting and fault-
1478   controlled sedimentation in the Triassic deposits of Eastern Svalbard, Norwegian Petroleum
1479   directorate Bulletin, 10, 61–79, 2014.

1480 Petersen, T. G., Thomsen, T. B., Olaussen, S. and Stemmerik, L.: Provenance shifts in an evolving
1481   Eurekan foreland basin: the Tertiary Central Basin, Spitsbergen, J. Geol. Soc., London, 173,
1482   634–648, 2016.

1483 Peucat, J.-J., Ohta, Y., Gee, D. G. and Bernard-Griffiths, J.: U-Pb, Sr and Nd evidence for
1484   Grenvillian and latest Proterozoic tectonothermal activity in the Spitsbergen Caledonides,
1485   Arctic Ocean, Lithos, 22, 275–285, 1989.

1486 Phillips, T., Jackson, C. A-L., Bell, R. E., Duffy, O. B. and Fossen, H.: Reactivation of
1487   intrabasement structures during rifting: A case study from offshore southern Norway,
1488   Journal of Structural Geology, 91, 54–73, 2016.

1489 Piepjohn, K.: The Svalbardian–Ellesmerian deformation of the Old Red Sandstone and the pre-
1490   Devonian basement in NW Spitsbergen (Svalbard), in: New Perspectives on the Old Red
1491   Sandstone, edited by: Friend, P. F. and Williams, B. P. J., Geol. Soc. London Spec. Publi.,
1492   180, 585–601, 2000.

1493 Piepjohn, K.: von Gosen, W., Läufer, A., McClelland, W. C. and Estrada, S.: Ellesmerian and
1494   Eurekan fault tectonics at the northern margin of Ellesmere Island (Canadian High Arctic),
1495   Z. Dt. Ges. Geowiss., 164, 1, 81–105, 2013.

1496 Piepjohn, K., Dallmann, W. K. and Elvevold, S.: The Lomfjorden Fault Zone in eastern Spitsbergen
1497   (Svalbard), in: Circum-Arctic Structural Events: Tectonic Evolution of the Arctic Margins
1498   and Trans-Arctic Links with Adjacent Orogens, edited by: Piepjohn, K., Strauss, J. V.,
1499   Reinhardt, L. and McClelland, W. C., GSA Spec. Paper, 541, 95–130, 2019.

1500 Ramsay, J. G.: Interference Patterns Produced by the Superposition of Folds of Similar Type, J.
1501   Geol., 70, 4, 466–481, 1962.

1502 Rice, A. H. N.: Restoration of the External Caledonides, Finnmark, North Norway, in: New
1503   Perspectives on the Caledonides of Scandinavia and Related Areas, Corfu, F., Gasser, D.

and Chew, D. M. (eds), Geological Society, London, Special Publications, 390, 271-299, 2014.

Roberts, D.: Tectonic Deformation in the Barents Sea Region of Varanger Peninsula, Finnmark, Norges geol. unders., 282, 1–39, 1972.

Roberts, D. and Olovyanishshnikov, V.: Structural and tectonic development of the Timanide orogeny, in: The Neoproterozoic Timanide Orogen of Eastern Baltica, edited by: Gee, D. G. and Pease, V., Geol. Soc. London, Mem., 30, 47–57, 2004.

Roberts, D. and Siedlecka, A.: Timanian orogenic deformation along the northeastern margin of Baltica, Northwest Russia and Northeast Norway, and Avalonian-Cadomian connections, Tectonophysics, 352, 1r69-184, 2002.

Roberts, D. and Williams, G. D.: Berggrunnskart Kjøllefjord 2236 IV, M 1:50.000, foreløpig utgave, Norges geol. unders., 2013.

Roberts, D., Mitchell, J. G. and Andersen, T. B.: A post-Caledonian dyke from Magerøy North Norway: age and geochemistry, Norwegian Journal of Geology, 71, 289-294, 1991.

Rosa, D., Majka, J., Thrane, K. and Guarnieri, P.: Evidence for Timanian-age basement rocks in North Greenland as documented through U–Pb zircon dating of igneous xenoliths from the Midtkap volcanic centers, Precambrian Res., 275, 394–405, 2016.

Schiffer, C., Doré, A. G., Foulger, G. R., Franke, D., Geoffroy, L., Gernigon, L., Holdsworth, B., Kusznir, N., Lundin, E., McCaffrey, K., Peace, A. L., Petersen, K. D., Phillips, T. B., Stephenson, R., Stoker, M. S. and Welford, J. K.: Structural inheritance in the North Atlantic, Earth-Science Reviews, 206, 102975, 2020.

Senger, K., Roy, S., Braathen, A., Buckley, S., Bælum, K., Gernigon, L., Mjelde, R., Noormets, R., Ogata, K., Olaussen, S., Planke, S., Ruud, B. O. and Tveranger, J.: Geometries of doleritic intrusions in central Spitsbergen, Svalbard: an integrated study of an onshore-offshore magmatic province with applications to CO_2 sequestration, Norw. J. Geol., 93, 143–166, 2013.

Siedlecka, A.: Late Precambrian Stratigraphy and Structure of the North-Eastern Margin of the Fennoscandian Shield (East Finnmark – Timan Region), Nor. geol. unders., 316, 313-348, 1975.

1533   Siedlecka, A. and Roberts, D.: Report from a visit to the Komi Branch of the Russian Academy of
1534   Sciences in Syktyvkar, Russia, and from fieldwork in the central Timans, August 1995,
1535   Norges geol. unders. report, 95.149, 32 pp., 1995.

1536   Siedlecka, A. and Siedlecki, S.: Some new aspects of the geology of Varanger peninsula (Northern
1537   Norway), Nor. geol. unders., 247, 288-306, 1967.

1538   Siedlecka, A. and Siedlecki, S.: Late Precambrian sedimentary rocks of the Tanafjord–
1539   Varangerfjord region of Varanger Peninsula, Northern Norway, in: The Caledonian
1540   Geology of Northern Norway, edited by: Roberts, D. and Gustavson, M., Norges geol.
1541   unders., 269, 246–294, 1971.

1542   Smelror, M., Petrov, O. V., Larssen, G. B. and Werner, S. C.: Geological Atlas of the Barents Sea,
1543   Geological Survey of Norway, Trondheim, Norway, 2009.

1544   Smyrak-Sikora, A., Osmundsen, P. T., Braathen, A., Ogata, K., Anell, I., Mulrooney, M. J. and
1545   Zuchuat, V: Architecture of growth basins in a tidally influenced, prodelta to delta-front
1546   setting: The Triassic succession of Kvalpynten, East Svalbard, Basin Research, 32, 5, 959–
1547   988, 2020.

1548   Stouge, S., Christiansen, J. L. and Holmer, L. E.: Lower Palaeozoic stratigraphy of
1549   Murchisonfjorden and Sparreneset, Nordaustlandet, Svalbard, Geografiska Annaler: Series
1550   A, Physical Geography, 93, 209–226, 2011.

1551   Sturt, B. A., Pringle, I. R. and Ramsay, D. M.: The Finnmarkian phase of the Caledonian Orogeny,
1552   J. Geol., Soc., London, 135, 597–610, 1978.

1553   Thiede, J., Pfirman, S., Schenke, H.-W. and Reil, W.: Bathymetry of Molloy Deep: Fram Strait
1554   Between Svalbard and Greenland, Mar. Geophys. Res., 12, 197–214, 1990.

1555   Tonstad, S. A.: The Late Paleozoic development of the Ottar basin from seismic 3D interpretation,
1556   Master's Thesis, University of Tromsø, Tromsø, Norway, 135 pp., 2018.

1557   Torsvik, T. H. and Trench, A.: The Ordovician history of the Iapetus Ocean in Britain: new
1558   palaeomagnetic constraints, J. Geol. Soc., London, 148, 423–425, 1991.

1559   Torsvik, T. H., Burke, K., Steinberger, B., Webb, S. J. and Ashwal, L. D.: Diamond sampled by
1560   plumes from the core–mantle boundary, Nature Lett., 466, 352–355, 2010.

1561   Townsend, C.: Thrust transport directions and thrust sheet restoration in the Caledonides of
1562   Finnmark, North Norway, J. Structural Geol., 9, 3, 345–352, 1987.

1563   Vernikovsky, V. A., Metelkin, D. V., Vernikovskaya, A. E., Matushkin, N. Yu., Lobkovsky, L. I.

1564   and Shipilov, E. V.: Early evolution stage of the arctic margins (Neoproterozoic-Paleozoic)

1565   and plate reconstructions, ICAM VI Proceedings, May 2011, Fairbanks, Alaska, USA, 265–

1566   285, 2011.

1567   Von Gosen, W. and Piepjohn, K.: Polyphase Deformation in the Eastern Hornsund Area, Geol. Jb.,

1568   B91, 291–312, 2001.

1569   Witt-Nilsson, P., Gee, D. G. and Hellman, F. J.: Tectonostratigraphy of the Caledonian Atomfjella

1570   Antiform of northern Ny Friesland, Svalbard, Norsk Geol. Tidsskr., 78, 67–80, 1998.

1571   Worsley, D., Agdestein, T., Gjelberg, J. G., Kirkemo, K., Mørk, A., Nilsson, I., Olaussen, S., Steel,

1572   R. J. and Stemmerik, L.: The geological evolution of Bjørnøya, Arctic Norway:

1573   implications for the Barents Shelf, Norsk Geol. Tidsskr., 81, 195–234, 2001.

1574   Ziegler, P. A.: Evolution of the Arctic–North Atlantic and the Western Tethys, AAPG Mem. 43,

1575   1988.

1576

1577 **Figures**

1578
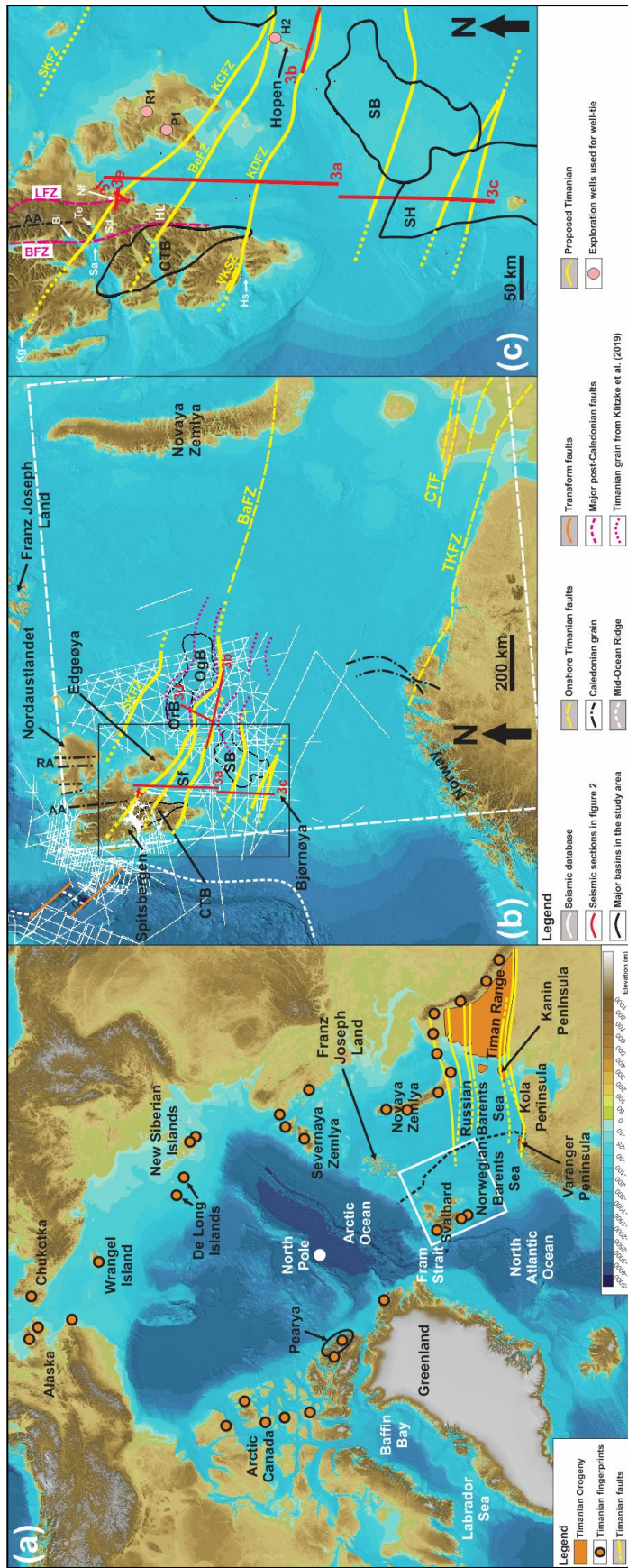
Figure 1: (a) Overview map showing the Timanian belt in Russia and Norway, and occurrences of Timanian fingerprints throughout the Arctic; (b) Regional map of Svalbard and the Barents Sea the main geological elements and the seismic database used in the present study. The location of (b) is shown as a white frame in (a); (c) Zoom in the northern Norwegian Barents Sea and Svalbard showing the main faults and basins in the study area, and the proposed Timanian structures. The location of (c) is shown as a black frame in (b). The location of the Raddedalen-1 well is from Smyrak-Sikora et al. (2020). Topography and bathymetry are from Jakobsson et al. (2012). Abbreviations: AA: Atomfjella Antiform; BaFZ: Baidaratsky fault zone; BeFZ: Bellsundbanken fault zone; BFZ: Billefjorden Fault Zone; Bi: Billefjorden; CTB: Central Tertiary Basin; HL: Heer Land; Hs: Hornsund; H2: Hopen-2; KCFZ: Kongsfjorden–Cowanodden fault zone; KDFZ: Kinnhøgda–Daudbjørnpynten fault zone; Kg: Kongsfjorden; LFZ: Lomfjorden Fault Zone; Nf: Nordmannsfonna; OgB: Olga Basin; OrB: Ora Basin; P1: Plurdalen-1; RA: Rijpdalen Anticline; R1: Raddedalen-1; Sa: Sassenfjorden; SB: Sørkapp Basin; Sf: Storfjorden; SH: Stappen High; SKFZ: Steiløya–Krylen fault zone; Te: Tempelfjorden; TKFZ: Trollfjorden–Komagelva Fault Zone; VKSZ: Vimsodden–Kosibapasset Shear Zone.
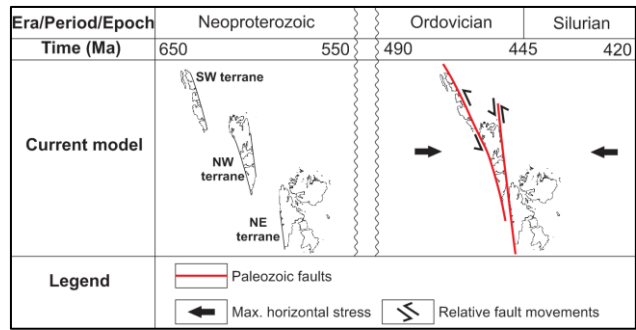
1591

1592 Figure 2: Paleogeographic reconstruction of the Svalbard Archipelago in the latest Neoproterozoic during the Timanian
1593 Orogeny and in the early–mid Paleozoic during the Caledonian Orogeny according to previous models (e.g., Harland, 1969;
1594 Labrousse et al., 2008).

1595

1596

1597

1598
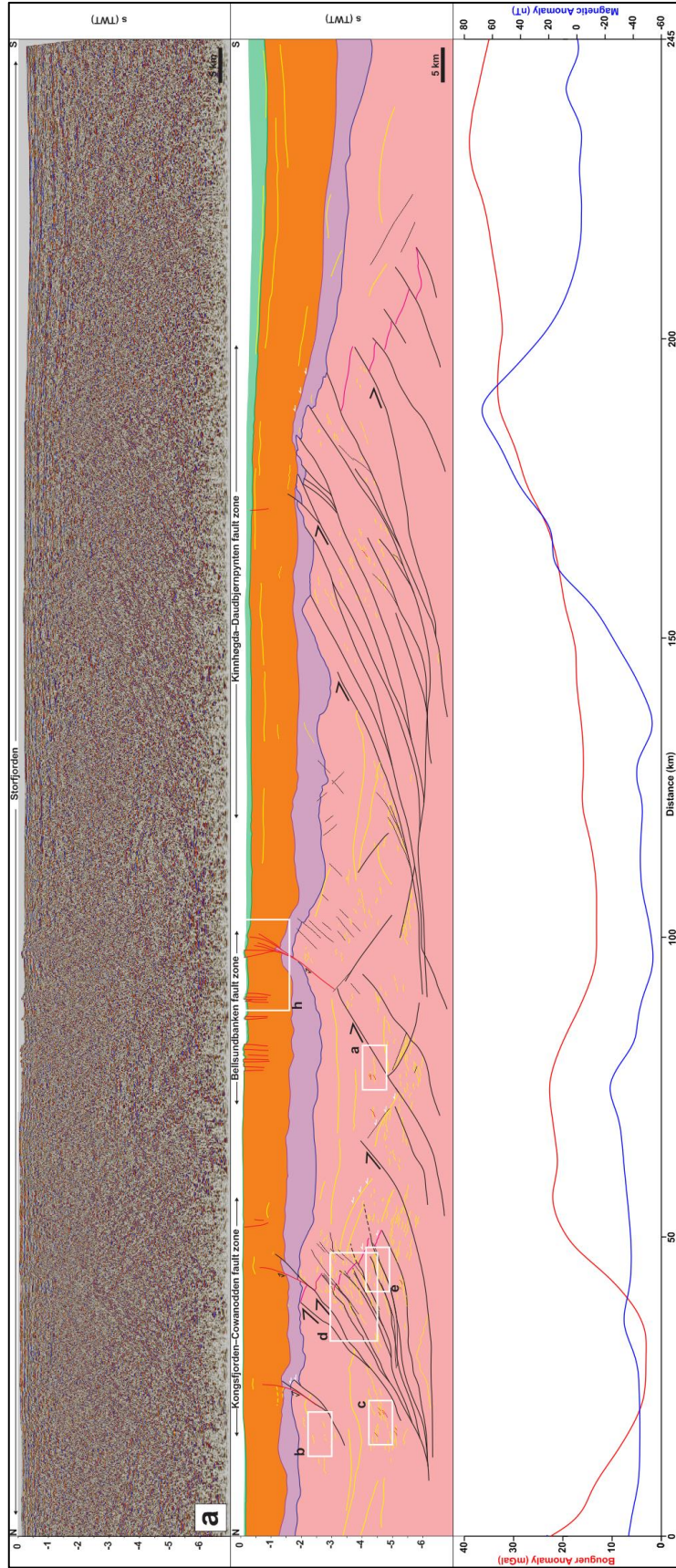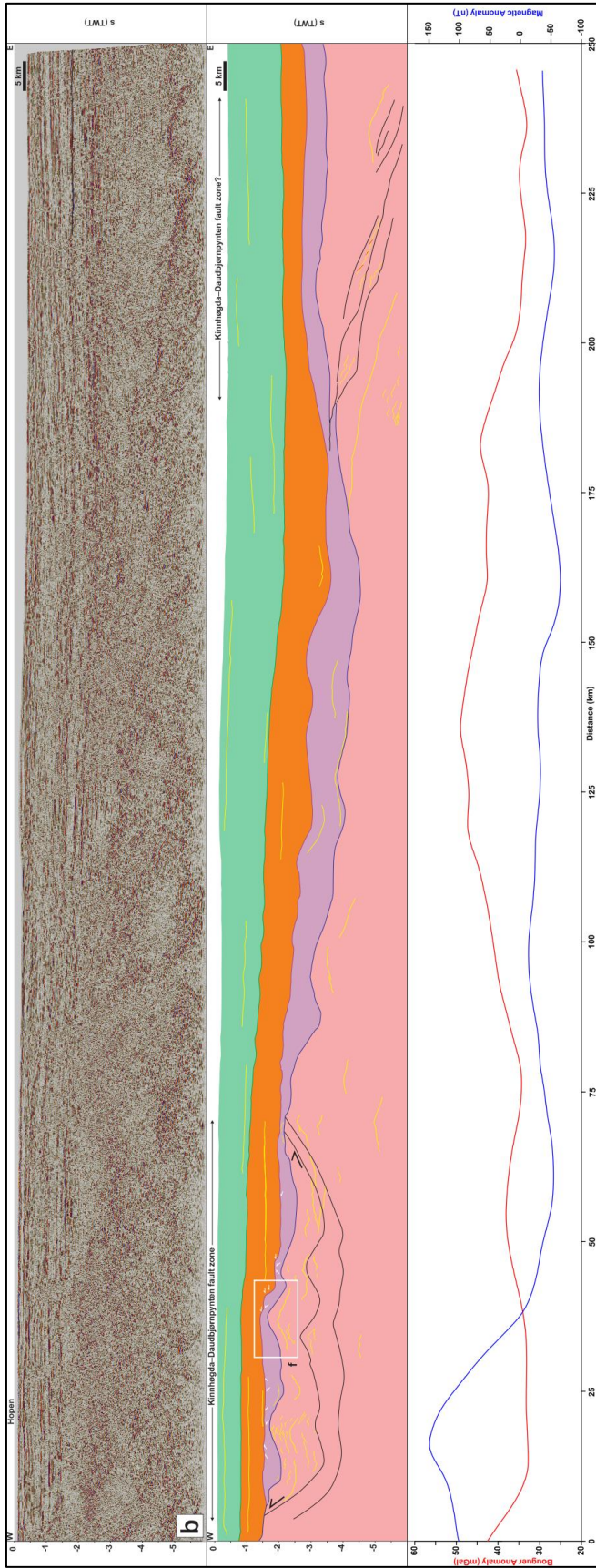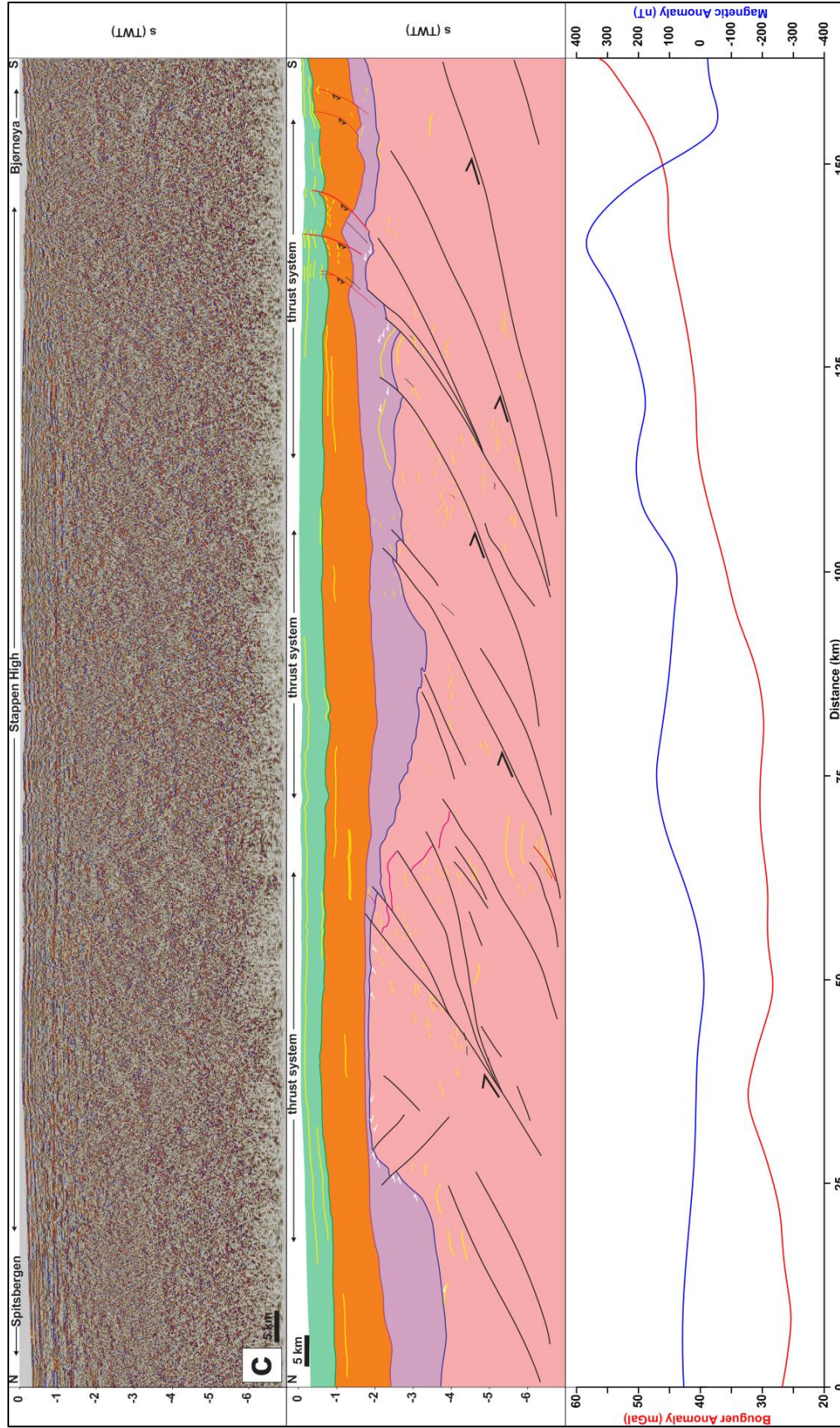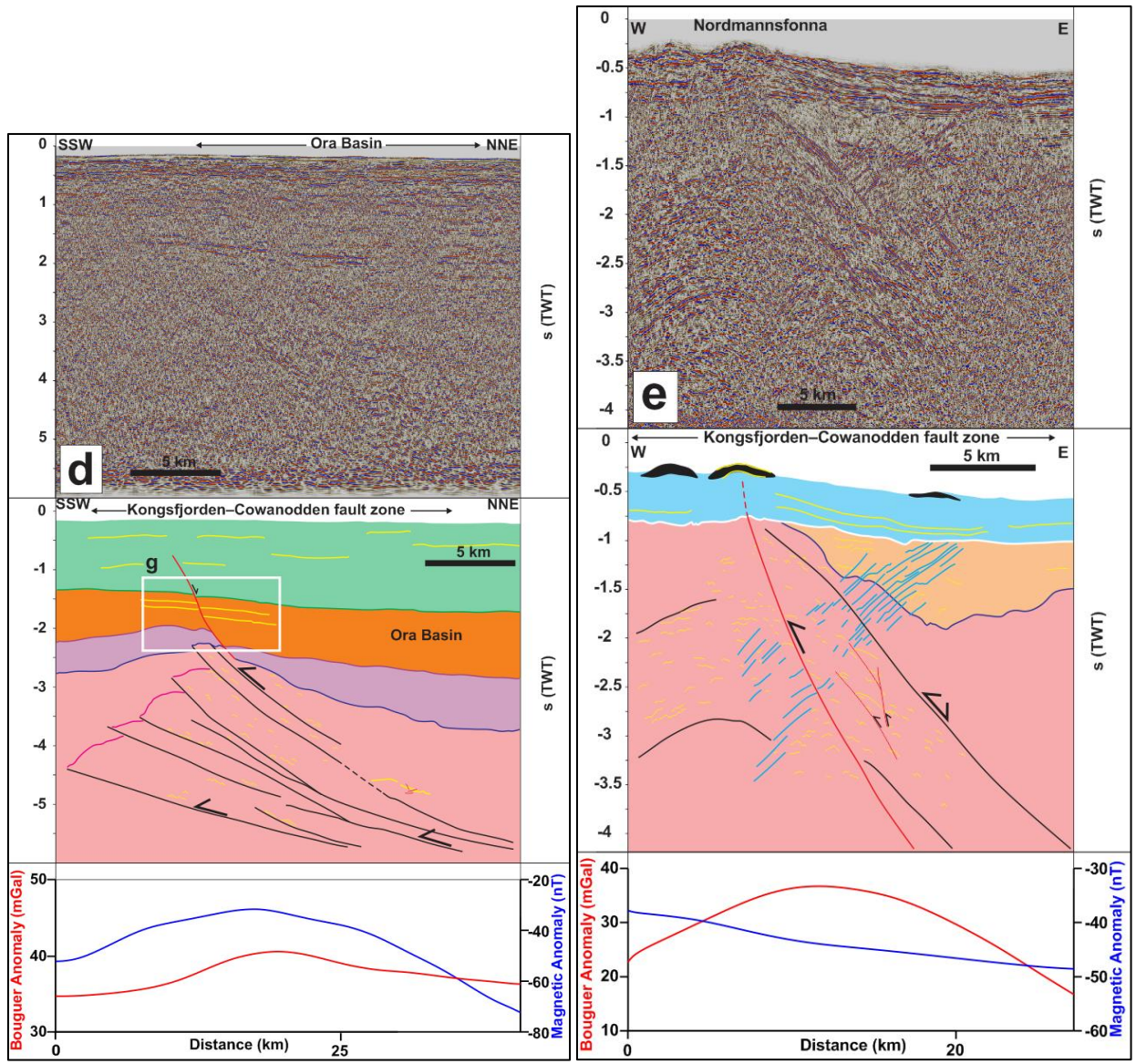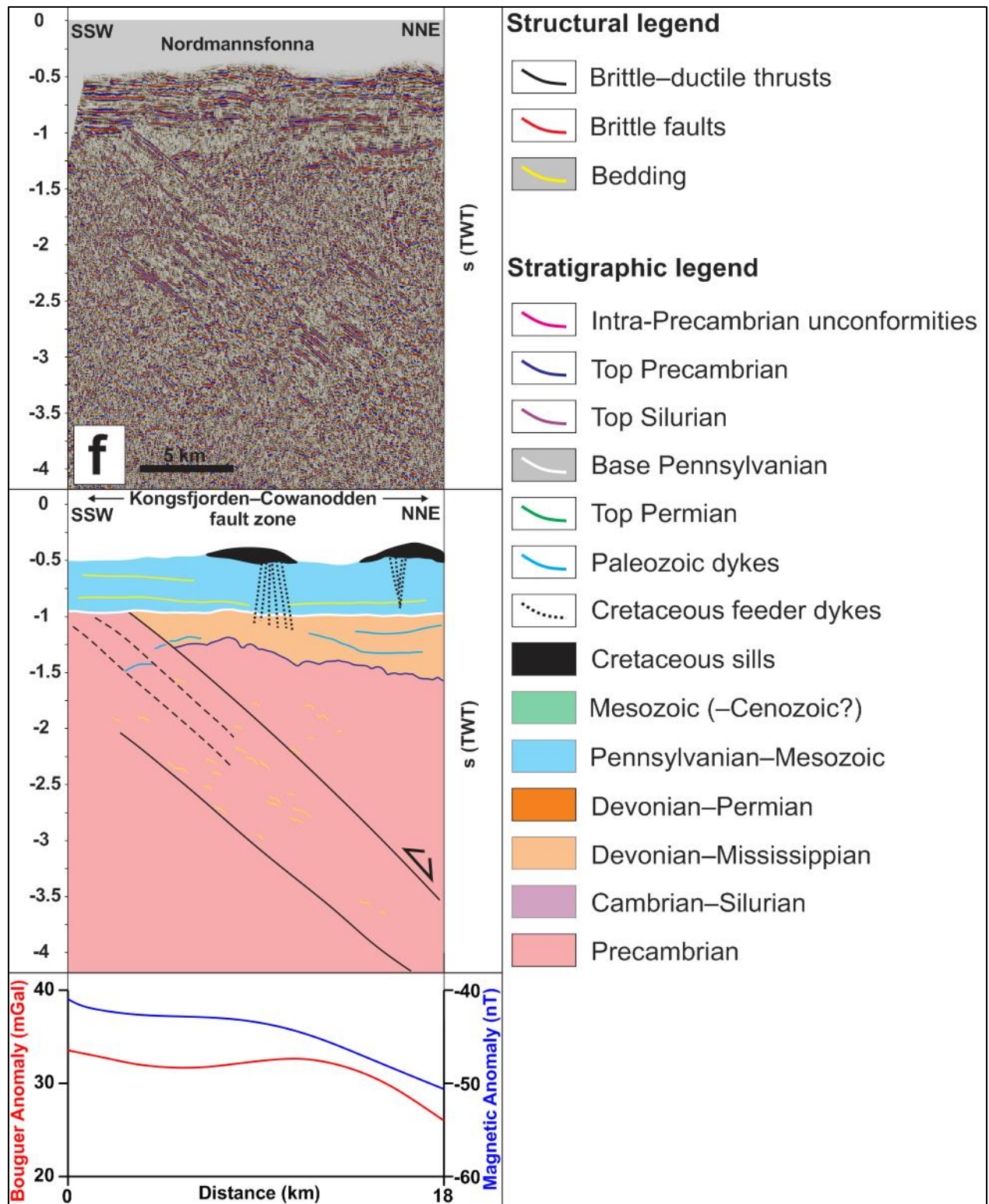
1599

Figure 3: Interpreted seismic profiles and associated potential field data (a) in Storfjorden, (b) south of Hopen, (c) on the
Stappen High in the northwestern Norwegian Barents Sea between Spitsbergen and Bjørnøya, (d) on the southern flank of
the Ora Basin in the northeastern Norwegian Barents Sea, and (e and f) in Nordmannsfonna in eastern Spitsbergen. The
seismic profiles show top-SSW Timanian thrusts that were reactivated and overprinted during subsequent tectonic events
such as Caledonian contraction, Devonian–Carboniferous late–post Caledonian collapse and rifting, Eurekan contraction,
and present-day contraction. Profiles (e) and (f) also show Paleozoic and Cretaceous intrusions. The white frames show the

1606   location of zoomed-in portions of the profiles displayed in Figure 4. Potential field data below the seismic profiles include
1607   Bouguer anomaly (red lines) and magnetic anomaly (blue lines). The potential field data show consistently high gravimetric
1608   anomalies and partial correlation with high magnetism towards the footwall of each major thrust systems (i.e., towards
1609   thickened portions of the crust).

1610
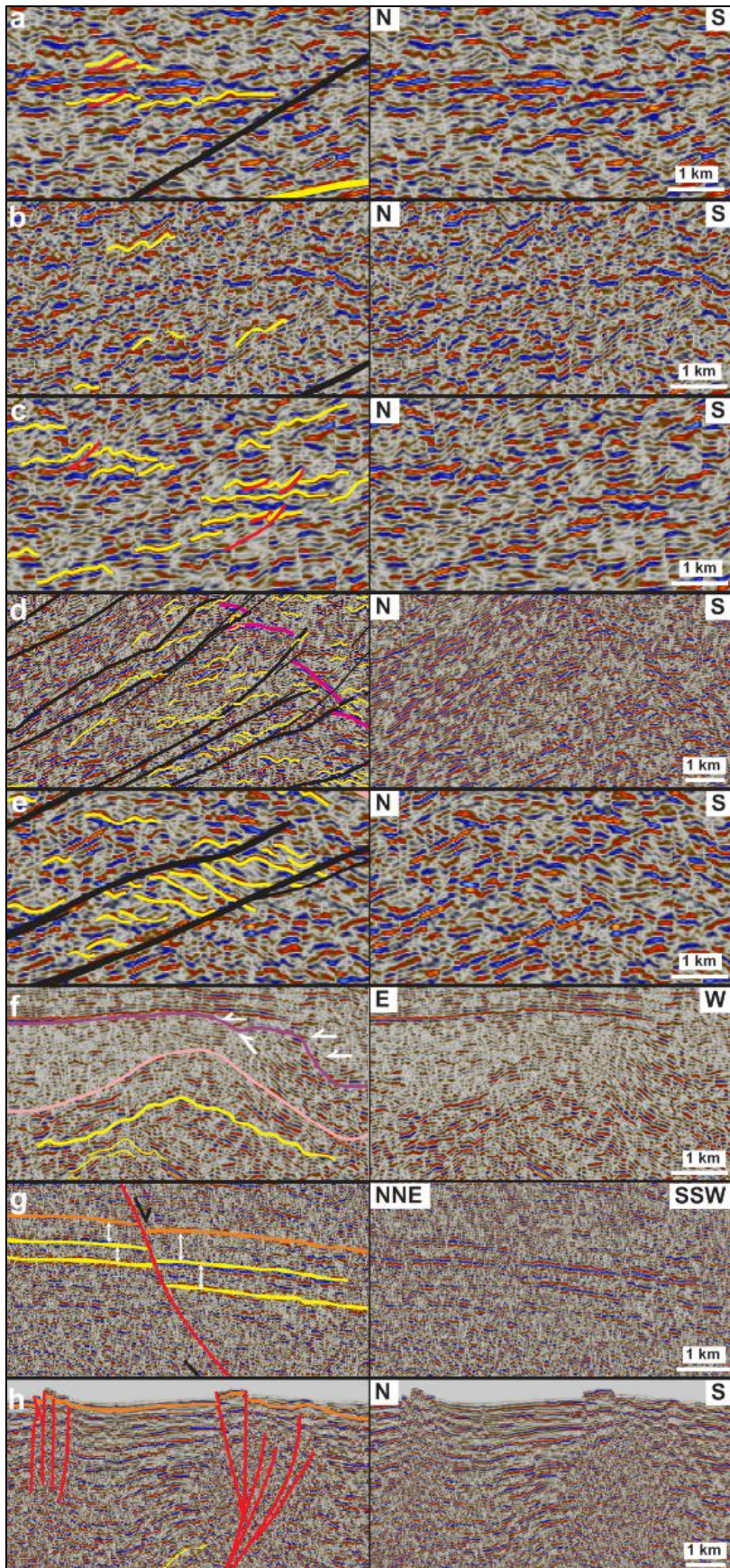
1612 **Figure 4: Zooms in seismic profiles shown in Figure 3 showing (a) upright fold structures, (b) SSW-verging folds and (c)**
1613 **top-SSW minor thrusts in Precambrian–lower Paleozoic (meta-) sedimentary basement rocks, (d) SSW-verging folds and**
1614 **NNE-dipping mylonitic shear zones within a major thrust that offsets major basement unconformities (fuchsia lines) top-**
1615 **SSW, (e) duplex structures within a major top-SSW thrust, (f) a N–S- to NNE–SSW-trending, 5–15 kilometers wide,**
1616 **symmetrical , upright macro-fold and associated, kilometer- to hundreds of meter-scale, parasitic macro- to meso-folds, (g)**
1617 **syn-tectonic thickening in Devonian–Carboniferous (–Permian?) sedimentary strata offset down-NNE by a normal fault**
1618 **that merges with a thick mylonitic shear zone at depth, and (h) recent–ongoing reverse offsets of the seafloor reflection by**
1619 **multiple, inverted, NNE-dipping normal faults in Storfjorden. See Figure 3 for location of each zoom and for legend.**

1620

1621
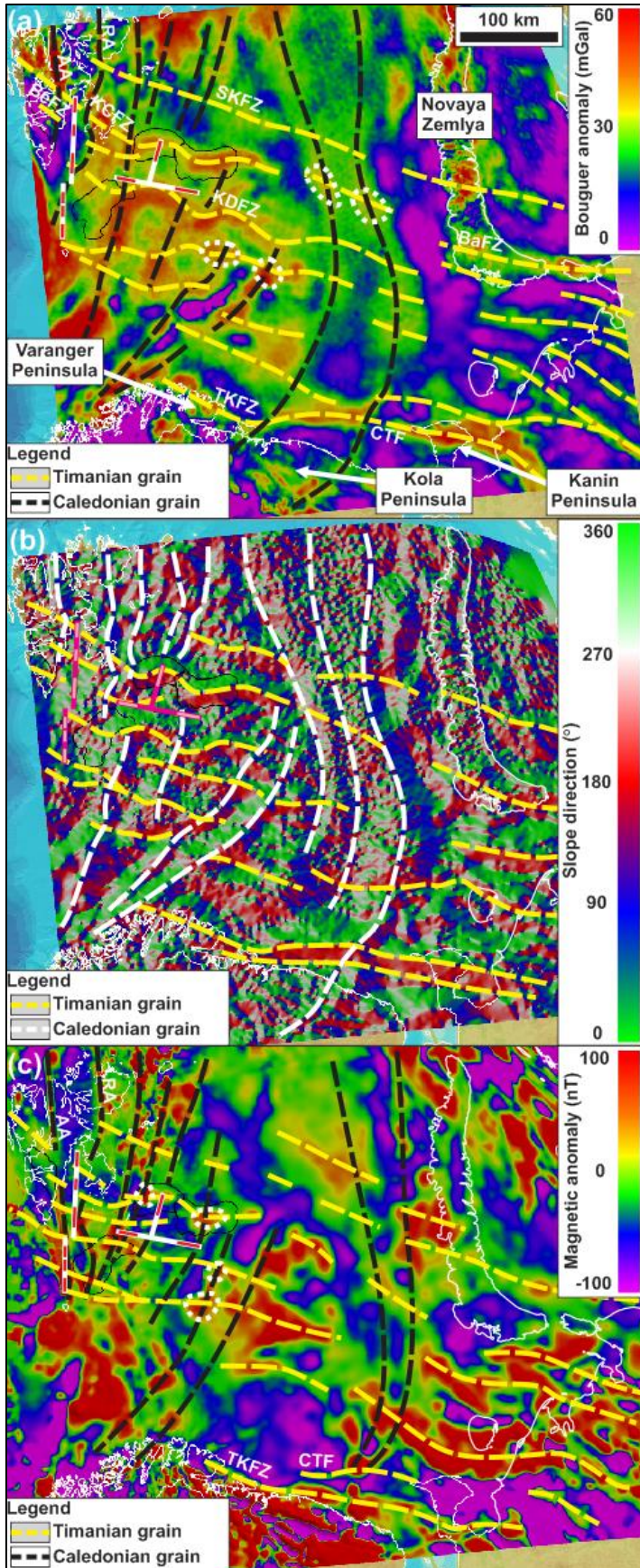
Figure 5: Gravimetric (a and b) and magnetic (c) anomaly maps over the Barents Sea and adjacent onshore areas in Russia (see location as a dashed white frame in Figure 1b), Norway and Svalbard showing E–W- to NW–SE-trending anomalies (dashed yellow lines) that correlate with the proposed NNE-dipping Timanian thrust systems in Svalbard and the northern Norwegian Barents Sea. Note the high obliquity of E–W- to NW–SE-trending Timanian grain with NE–SW- to N–S-trending Caledonian grain (dashed black/white lines). Note that dashed lines in (a) and (c) denote high gravimetric and magnetic anomalies. Also notice the oval-shaped high gravimetric and magnetic anomalies (dotted white lines) at the intersection of WNW–ESE- and N–S- to NNE–SSW-trending anomalies in (a) and (c) resulting from the interaction of the two (Timanian and Caledonian) thrust and fold trends. The location of seismic profiles presented in Figure 3a–d are shown as thick white lines in (a) and (c) and as fuchsia lines in (b). Within these thick white and fuchsia lines, the location and extent of thrust systems evidenced on seismic data (Figure 3) is shown in white in (a) and (c) and in pink in (b). For the E–W-trending seismic profile shown in Figure 3b, this implies that the red and pink lines represent N–S-trending synclines. Abbreviations: AA: Atomfjella Antiform; BaFZ: Baidaratsky fault zone; BeFZ: Bellsundbanken fault zone; CTF: Central Timan Fault; KCFZ: Kongsfjorden–Cowanodden fault zone; KDFZ: Kinnhøgda–Daudbjørnpynten fault zone; RA: Rijpdalen Anticline; SKFZ: Steiløya–Krylen fault zone; TKFZ: Trollfjorden–Komagelva Fault Zone.

1637
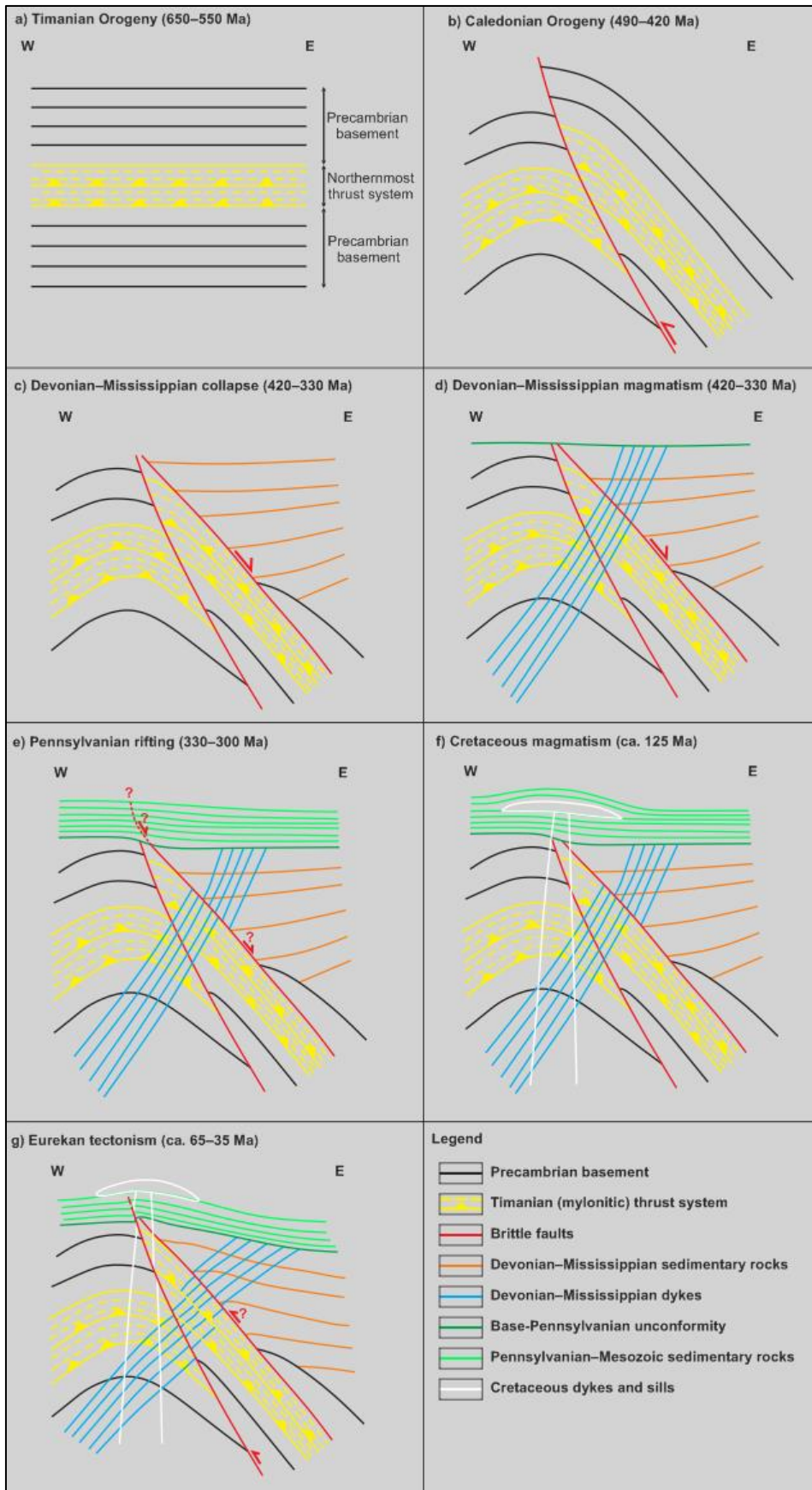
Figure 6: Sketches showing a possible reconstruction of the tectonic history of the E–W seismic profile in Nordmannsfonna shown in Figure 3e. (a) Formation of a NNE-dipping, mylonitic thrust system (Kongsfjorden–Cowanodden fault zone) within Precambrian basement rocks during the Timanian Orogeny in the latest Neoproterozoic. The NNE-dipping Kongsfjorden–Cowanodden fault zone appears near horizontal on the E–W transect; (b) Top-west thrusting along the east-dipping Agardhbukta Fault and folding of the Kongsfjorden–Cowanodden fault zone into a broad, moderately NNE-plunging anticline during the Caledonian Orogeny; (c) Inversion of the Kongsfjorden–Cowanodden fault zone along the eastern flank of the Caledonian anticline and deposition of thickened, gently west-dipping, syn-tectonic, Devonian (–Mississippian?) sedimentary strata during post-Caledonian collapse-related extension; (d) Intrusion of Precambrian basement and Devonian (–Mississippian?) sedimentary rocks by steeply west-dipping dykes in the Devonian–Mississippian; (e) Regional erosion in the mid-Carboniferous (latest Mississippian) and deposition of Pennsylvanian sedimentary strata, possibly along a high-angle brittle splay of the inverted portion of the Kongsfjorden–Cowanodden fault zone during rift-related extension; (f) Deposition of Mesozoic sedimentary strata and intrusion of Cretaceous dolerite dykes and sills; (g) Erosion of Pennsylvanian–Mesozoic strata and reactivation of the Kongsfjorden–Cowanodden fault zone and Agardhbukta Fault with minor reverse movements in the early Cenozoic during the Eurekan tectonic event as shown by mild folding and offset of overlying post-Caledonian sedimentary strata, dykes and Base-Pennsylvanian unconformity. Also note the back-tilting (i.e., clockwise rotation) of Devonian–Mississippian dykes in the hanging wall of the Agardhbukta Fault and of the Kongsfjorden–Cowanodden fault zone.

1656
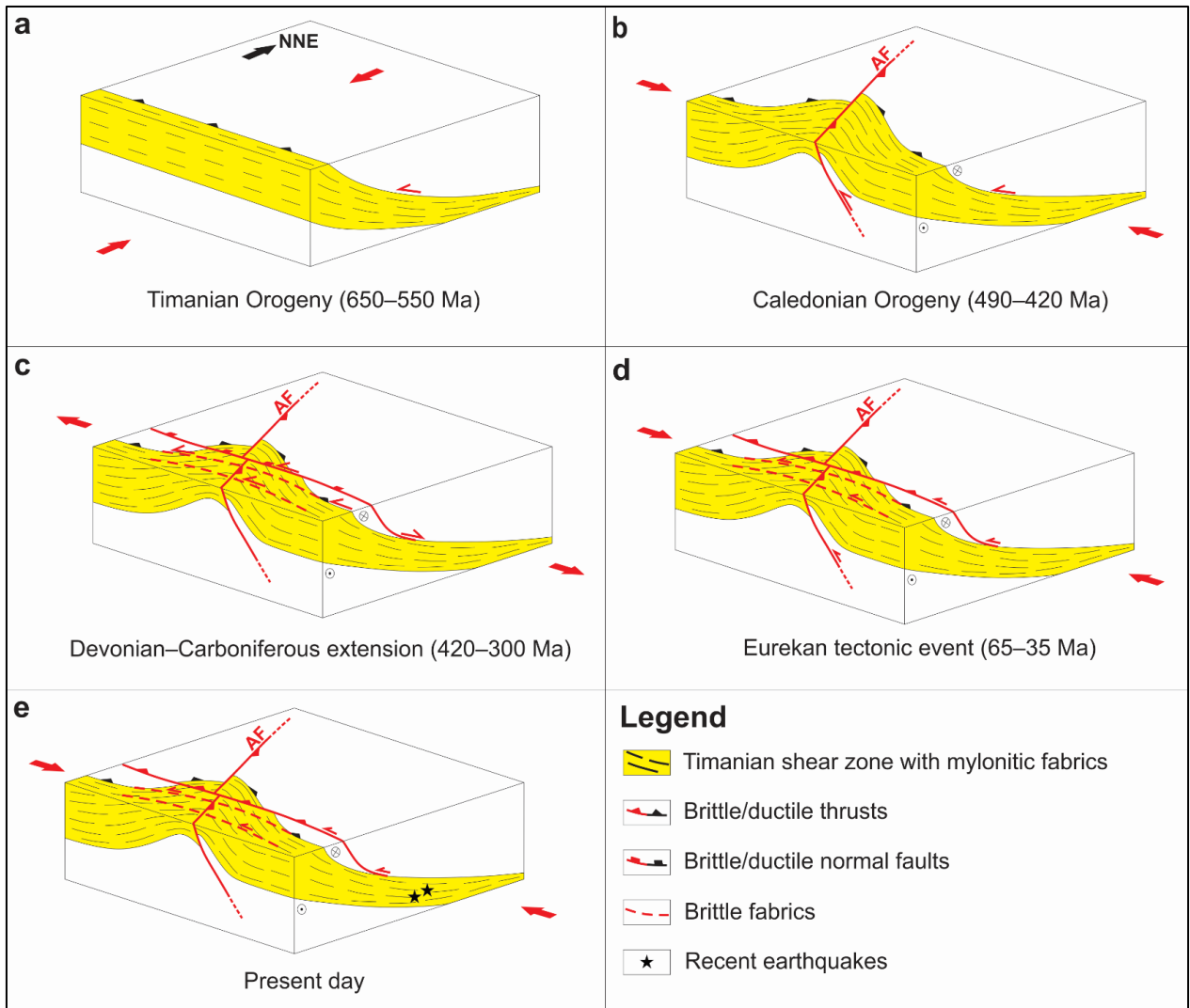
Figure 7: Tectonic evolution of Timanian thrust systems in eastern Spitsbergen, Storfjorden and the northwestern Norwegian Barents Sea including (a) top-SSW thrusting during the Timanian Orogeny, (b) reactivation as oblique-slip sinistral-reverse thrusts and offset by top-west brittle thrust overprints (e.g., Agardhbukta Fault – AF) under E–W contraction during the Caledonian Orogeny, (c) reactivation as low-angle, brittle–ductile, normal–sinistral extensional detachments and overprinting by high-angle normal–sinistral brittle faults during Devonian–Carboniferous, late–post-Caledonian extensional collapse and rifting, (d) reactivation as brittle–ductile sinistral–reverse thrusts, overprinting by high-angle sinistral–reverse brittle thrusts, and mild offset by reactivated top-west thrusts (e.g., Agardhbukta Fault – AF) during E–W Eurekan contraction, and (e) renewed, recent–ongoing, sinistral–reverse reactivation and overprinting possibly due to ongoing magma extrusion and transform faulting (ridge-push?) in the Fram Strait.

1666

Era/Period/Epoch	Neoproterozoic	Ordovician	Silurian
Time (Ma)	650 550	490 445	420
Model proposed			
Legend			

Legend: Paleozoic faults — Timanian thrusts ···· — Max. horizontal stress — Relative fault movements
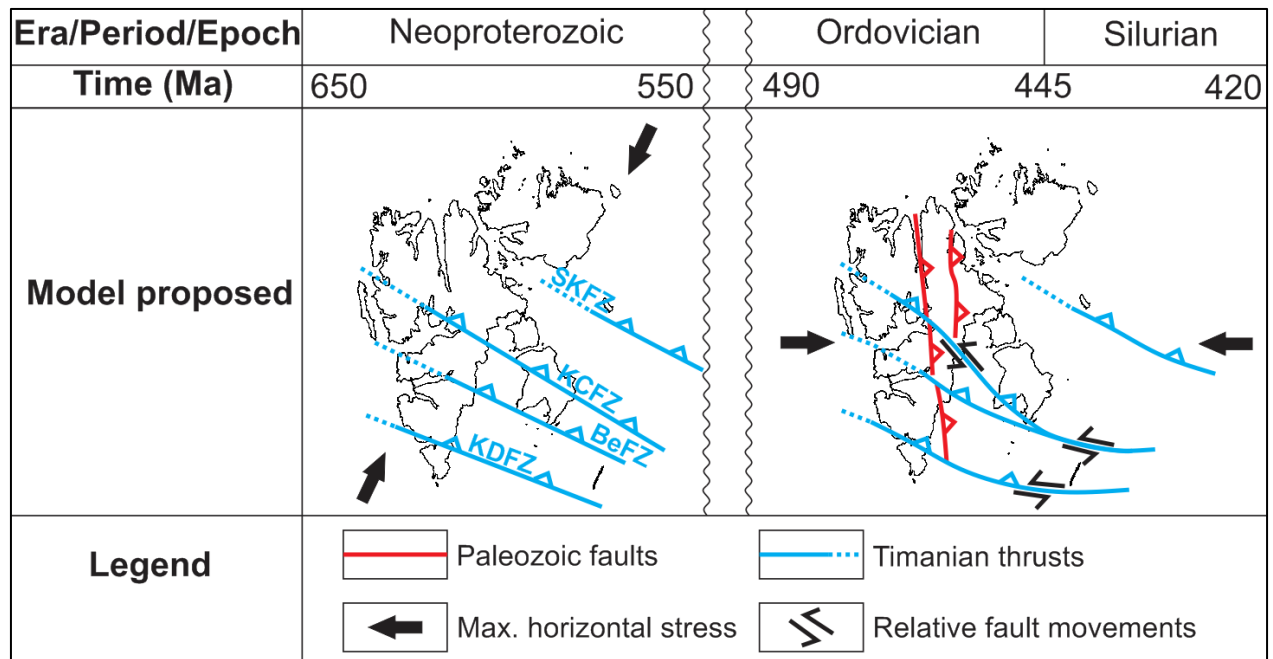
Figure 8: Paleogeographic reconstruction of the Svalbard Archipelago in the latest Neoproterozoic during the Timanian Orogeny and in the early–mid Paleozoic during the Caledonian Orogeny according to the present study.